Phase Transitions in a Model of Interacting Anharmonic Oscillators

T. R. Koehler
IBM Research Laboratory, San Jose, California 95114

N. S. Gillis*
Sandia Laboratories, Albuquerque, New Mexico 87115

(Received 20 November 1972)

As a prototype of a ferroelectric crystal we consider a system of interacting anharmonic oscillators. This model is treated via a simple Hamiltonian which consists of a sum of single-particle quartic-anharmonic-oscillator Hamiltonians together with a quadratic intercell interaction term. The interaction term—typically long range in nature—is treated in a molecular-field approximation, yielding an effective lattice Hamiltonian which can be scaled in terms of two parameters only—an effective-inverse-mass parameter and an effective coupling strength. For computational simplicity we treat the inverse-mass parameter as an effective temperature, with zero-point fluctuations playing the role of thermal fluctuations. The effective lattice Hamiltonian is solved numerically exactly to determine whether the lattice of coupled oscillators will, at some temperature, undergo a transition to a state in which the average value of the particle displacement is nonzero. From the properties of the exact solution it is shown that one can have a second-order transition or no transition, depending on the magnitude of the intercell coupling. If the anharmonic potential in which each particle moves possesses a double-well character, a second-order transition will occur for any value of the coupling strength greater than zero. On the other hand, if the anharmonic potential exhibits only a single minimum, then a transition will occur only if the coupling strength exceeds a critical value. These and other exact results establish a basis for ascertaining the range of validity of certain approximate treatments of the molecular-field Hamiltonian. In particular, we discuss in detail (i) variational treatments in which a set of trial displaced-oscillator wave functions are introduced as solutions to the molecular-field Hamiltonian and (ii) a so-called "two-level" approximation which is analogous to the de Gennes pseudospin model of hydrogen-bonded ferroelectrics. Finally, we discuss the collective properties of the system of coupled oscillators within the context of both the exact and approximate treatments.

I. INTRODUCTION

The past few years have seen an abundance of experimental information become available relating to lattice structural transformations in ferroelectric crystals, In particular, light scattering and inelastic neutron scattering have provided an insight into the dynamical aspects of these transitions which was heretofore unavailable. One broad conclusion which has evolved from the experimental investigations is that the traditional method of classifying ferroelectrics into one or the other of the categories of "order-disorder" or "displacive" is no longer valid. Indeed, most ferroelectric crystals probably reside somewhere between these two extremes. The early theoretical treatments of ferroelectrics were directed at either the order-disorder limit[1-7] or the displacive limit,[8-14] with little attempt being made to bridge the gap between the two extremes. More recently, however, progress has been made in this direction with the treatment of simplified model Hamiltonians which are capable of exhibiting qualitative behavior reminiscent of both the order-disorder and the displacive descriptions.[15,16]

For the most part, the theoretical treatments of structural transformations in ferroelectrics have centered about a lattice-dynamical approach which utilizes a crystal Hamiltonian of the schematic form

$$H = K + V_2 + V_3 + V_4 + \cdots .$$

Here K represents the kinetic-energy operator for all the ions in the crystal, whereas the terms V_n arise from a Taylor-series expansion of the effective interionic potential in powers of the ion displacements. The quadratic term V_2 is the usual harmonic term and contains contributions from both a short-range repulsive interaction and a longer-range dipolar interaction. The cubic and quartic anharmonic interactions V_3 and V_4 are usually assumed to be dominated by the short-range forces only.

From the microscopic viewpoint the ferroelectric crystal is distinguished from other insulating crystals by the fact that a long-wavelength cancellation occurs between the short-range repulsive interaction and the long-range dipolar interaction, giving rise to the so-called "polarization catastrophe." In particular, the force-constant matrix obtained from V_2 may be negative definite, so that the harmonic approximation represents an unstable state of equilibrium for the crystal. The crystal must then be stabilized by the V_4 interaction, with

the V_3 term giving rise to a coupling to the strain field. Clearly, if $V_2 < 0$ the inclusion of the V_4 interaction cannot be carried out using ordinary perturbative techniques which employ the harmonic approximation as a starting point. Furthermore, if the anharmonicities are particularly strong, as in the order-disorder ferroelectrics, perturbative techniques fail also. Thus, a self-consistent renormalization procedure must be devised which circumvents the harmonic approximation altogether. Recently, several such renormalization schemes have appeared on the theoretical scene[17–22] and have been applied with varying degrees of success to the description of lattice structural transformations in ferroelectric crystals.

In the present work we will be concerned with the solution of a model molecular-field Hamiltonian describing a system of interacting anharmonic oscillators. The model will be solved exactly using numerical procedures and the results compared with certain approximate self-consistent renormalization schemes. A primary point of concern will be how the order of the phase transition depends not only on the model parameters employed but also on the method of approximation. This will provide us with considerable insight into the validity of some of the recently employed approximation schemes for describing structural transitions in ferroelectrics.

We will be considering a periodic array of spherical anharmonic oscillators of inverse mass proportional to λ^2, one oscillator for each lattice cell l, coupled via a dipolarlike interaction bilinear in the lattice displacements. The system Hamiltonian will have the form

$$H=\sum_l \left(-\tfrac{1}{2}\lambda^2 \frac{d^2}{du_l^2} + \tfrac{1}{2} a u_l^2 + 4\varphi u_l^4 \right) - \frac{1}{2} \sum_{ll'} \chi(ll') u_l u_{l'} . \quad (1)$$

This Hamiltonian arises quite naturally if one considers the situation of a crystal consisting of two sublattices, with the atoms on one sublattice giving rise to a short-range intracell anharmonic single-particle potential in which the atoms of the second sublattice move. We can then imagine these latter atoms as being coupled via a long-range intercell dipolar interaction which is treated harmonically. Such a description provides a qualitative, but admittedly oversimplified, description of a prototype ferroelectric.

If the bilinear interaction term in (1) is truly long range in nature, then it should be a reasonable first approximation to treat the intercell interactions as a mean field, averaging over all cells except the cell of interest. Mathematically, this means that we approximate the density matrix of the entire crystal by a product of single-particle density matrices associated with the individual lattice cells, i.e.,

$$\rho(l_1, l_2, \ldots, l_N) \approx \prod_{m=1}^{N} \rho(l_m) .$$

When this is done the system Hamiltonian assumes the form of a sum of independent effective single-particle Hartree Hamiltonians, each of which resembles a quartic anharmonic oscillator in the presence of a self-consistent linear symmetry-breaking field. Thus, in the mean-field approximation, all the relevant static properties of this system of interacting oscillators can be obtained from a self-consistent determination of the eigenfunctions and eigenvalues of the single-particle Hamiltonian[23]:

$$H(u) = -\tfrac{1}{2}\lambda^2 \frac{d^2}{du^2} + \tfrac{1}{2} a u^2 + 4\varphi u^4 - \chi u \langle u \rangle , \quad (2)$$

where χ denotes the $q=0$ Fourier component of $\chi(ll')$. Miller and Kwok[24] have shown that a Hamiltonian of the form (2) follows from a Hartree description of a two-sublattice crystal such as we have discussed above, with the average of the single-particle coordinate, $\langle u \rangle$, being taken with respect to a single-particle density matrix based on the Hartree Hamiltonian (2).

We will be considering whether the system of coupled oscillators discussed above will, at some temperature, undergo a transition to a state in which the average value of the particle coordinate is nonzero. When such a transition occurs, we will determine whether it is continuous or discontinuous and how the detailed features of the transition depend on the method of approximation used.[25] We proceed by reformulating the problem somewhat, i.e., we ask what happens to the system of particles if we vary $\hbar$ (λ is proportional to $\hbar$) rather than varying the temperature. This varies the zero point rather than the thermal motion in a system in which the frequency remains constant in the harmonic approximation. Thus, thermal fluctuations have been replaced by zero-point fluctuations and λ behaves like an effective temperature. This permits us to employ a computationally and conceptually simpler wave-function formalism, as opposed to a more complicated density-matrix formalism without any change in the qualitative results. Thus, we concern ourselves with the ground-state energy of the system rather than the free energy and view the particle distribution in terms of the ground-state wave function. We will speak of varying "temperature" or λ interchangeably.

In Sec. II we compute the eigenfunctions and eigenvalues of the quartic oscillator for a wide range of λ^2 values by numerically diagonalizing the Hamil-

tonian (2) in the absence of the symmetry-breaking field. From a consideration of the qualitative features of the ground-state wave function, we are then able to distinguish between two distinct regimes which will be termed the "order-disorder" and the "displacive" regimes.

A treatment of the full Hamiltonian (2) including the self-consistent mean field, yields the result that for the case in which each particle moves in an anharmonic double-well potential ($a<0$), a second-order transition will occur from a state with $\langle u\rangle \neq 0$ to a state with $\langle u\rangle = 0$, irrespective of the coupling strength χ. On the other hand, for $a>0$ each particle moves in an anharmonic single-well potential and a transition will occur only if the coupling strength χ exceeds a critical value. In this case, the system is in the displacive regime for all λ values.

For $a<0$ we consider the evolution of the ground-state wave function in the presence of the mean field for transitions occurring in the order-disorder (small-λ^2), displacive (large-λ^2), and intermediate-λ^2 regimes. The inclusion of the symmetry-breaking field is considered both approximately and exactly. In the small-λ^2 regime a "two-level" approximation is employed, i.e., an approximation in which the Hamiltonian (2) is diagonalized in the 2×2 subspace of the ground and the first-excited states of the quartic oscillator. Such an approximation is equivalent to the original de Gennes[2] pseudospin model of hydrogen-bonded ferroelectrics and has been considered more recently by Miller and Kwok[24] within the context of a Hartree description of the crystal lattice. Comparing the results of this approximation with the results of an exact diagonalization of (2), we find that such an approximation is valid only for very small values of the coupling strength χ, yielding qualitatively incorrect results otherwise. Progressing from the order-disorder regime to larger-λ^2 values, the two-level approximation becomes progressively worse. Using the results of the exact evaluation of (2) as a guide, we examine various approximations appropriate to the displacive regime—in particular, we consider a variational treatment in which a displaced harmonic-oscillator wave function is employed as a trial ground-state wave function. In the $a<0$ case, the variational treatment predicts a first-order transition always, although the transition becomes more second order in character as the coupling strength increases. This result is to be compared with the exact treatment which predicts a second-order transition irrespective of the magnitude of χ. However, in the exact treatment the second-order transition becomes increasingly sharp as $\chi \to 0$ so that in the small-χ regime the transition predicted by the exact solution is almost first order in character. In the large-χ regime the λ dependence of the order parameter yielded by the variational treatment agrees quite well with the behavior of the order parameter of the exact solution except in the immediate vicinity of the transition. Indeed, the approximate treatment predicts a first-order transition before the second-order transition point of the exact solution is reached.

As might be anticipated, the variational treatment of the $a>0$ case yields an order parameter whose λ dependence mirrors quite well the λ dependence of the exact order parameter, except in the region near the transition, where the approximate treatment predicts a second-order transition occurring somewhat before the second-order transition of the exact solution.

In Sec. IV the collective properties of the oscillator system are treated by computing the response of the lattice to an external field which couples linearly to the particle displacements. The response function obtained in this way exhibits a resonance at a characteristic frequency whose long-wavelength component vanishes at the second-order transition point. The behavior of this "soft mode" is discussed within the context of both the approximate and exact treatments.

Section V of the paper is devoted to an evaluation of the various approximation schemes in the light of the information gleaned from the exact numerical treatment. In particular, the origin of the first-order transition in the variational treatment of the case where the particle moves in a double-well potential will be discussed.

In a recent paper, Onodera[16] considers a system of coupled oscillators in the mean-field approximation. By treating the problem classically, this author is able to obtain a formal expression for the susceptibility of the undistorted phase ($\langle u\rangle = 0$) in terms of hypergeometric functions. From a consideration of the properties of the classical paraelectric susceptibility, Onodera concludes that a second-order transition occurs for the model described by (2). In contrast to this, the present work does not restrict itself primarily to the region above the transition. In fact, some of the most important features which distinguish order-disorder from displacive behavior are to be found in the λ dependence of the order parameter below the transition.

II. EIGENVALUE SPECTRUM OF QUARTIC OSCILLATOR

By means of the scale transformation $u \to [|a|/(8\varphi)]^{1/2}u$, $\lambda \to \varphi(8/|a|)^{3/2}\lambda$, and $\chi \to 2\chi/|a|$, the Hamiltonian (2) can be cast in a form which exhibits only two independent parameters: an effective inverse-mass parameter and an effective coupling strength. Thus, a mean-field treatment of the coupled-oscillator problem reduces to that of de-

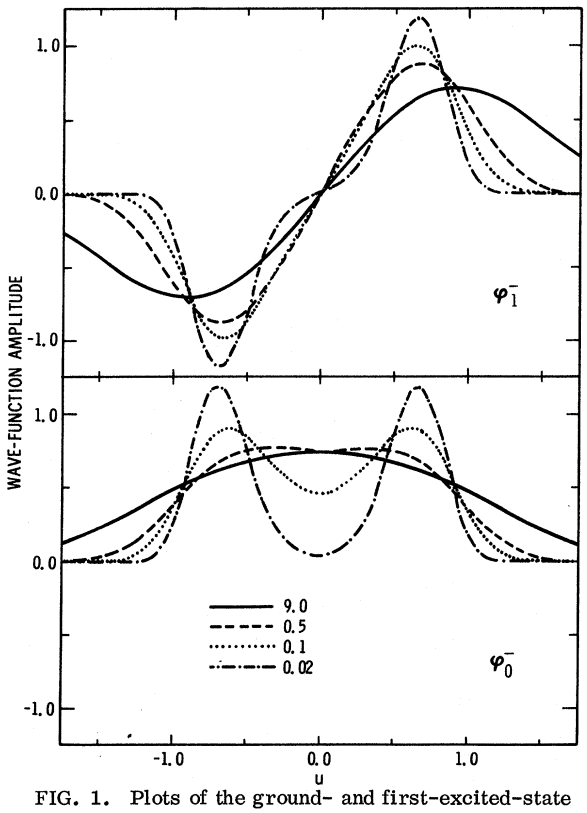

FIG. 1. Plots of the ground- and first-excited-state wave functions of $H_0^-(u)$. The curves are labeled by different values of λ^2.

termining the eigenvalue spectrum of the single-particle Hamiltonians

$$H^{\pm}(u) = H_0^{\pm}(u) - \chi u \langle u \rangle , \tag{3}$$

where

$$H_0^{\pm} \equiv -\tfrac{1}{2}\lambda^2 \frac{d^2}{du^2} \pm 4u^2 + 4u^4 .$$

In the present section we will be primarily concerned with the energy spectrum of $H_0^{\pm}(u)$. Since we are interested in including the anharmonicity exactly, we cannot rely on perturbative measures. On the other hand, since the eigenvalue spectrum of the quartic oscillator cannot be determined analytically, one must resort to a numerical diagonalization of $H_0^{\pm}(u)$ over a wide range of λ^2 values.

The numerical diagonalization is most easily implemented by constructing the Hamiltonian matrix $\langle n | H_0^{\pm} | n' \rangle$ using a set of basis states $|n\rangle$ which approximate as closely as possible the true eigenstates of $H_0^{\pm}$. For computational simplicity, a set of harmonic states would be desirable, although it is clear that the harmonic set derived from $H_0^{\pm}$ in the absence of the u^4 term is not the optimal set—indeed, for the case where the harmonic coefficient is negative, this basis is not even defined. Thus, we proceed by choosing a self-consistent set of basis states which include in some manner the anharmonicity of the u^4 term. Introducing a trial ground-state oscillator wave function of the form

$$|0\rangle = (g/\pi)^{1/4} e^{-gu^2/2}, \tag{4}$$

one can evaluate the ground-state expectation value of $H_0^{\pm}(u)$ as

$$E_0^{\pm} = \langle 0 | H_0^{\pm} | 0 \rangle = \tfrac{1}{4}\lambda^2 g \pm 2/g + 3/g^2 . \tag{5}$$

The extremal condition $\partial E_0^{\pm}/\partial g = 0$ then determines the variational parameter g as a solution to the cubic equation

$$\lambda^2 g^3 \mp 8g - 24 = 0 . \tag{6}$$

Of the three solutions to (6) only one corresponds to a true minimum of $E_0^{\pm}$. Using this choice for g it is then an easy matter to construct the complete set of oscillator states to be used in setting up the Hamiltonian matrix. The energy spectrum of these variational oscillator states will be denoted by $E_n^{\pm}$. In contrast to this, the energy and eigenfunction spectrum associated with the exact treatment of $H_0^{\pm}(u)$ will be denoted by $\mathcal{E}_n^{\pm}$ and $\varphi_n^{\pm}$.

In Fig. 1 the true ground-state and first-excited-state wave functions of $H_0^-(u)$ are plotted for a range of λ^2 values extending from 0.02 to 9. For small values of λ^2 these wave functions resemble symmetric and antisymmetric combinations, respectively, of Gaussian distributions centered at the minima of the double-well potential. In fact, the exact $\lambda^2 \to 0$ limit reduces the ground state of the system to a single doubly degenerate level with eigenvalue $\mathcal{E}_0^- = -1$, the wave functions consisting of a sum and difference of δ-function spikes centered at the positions of the potential minima. As the magnitude of λ^2 is increased the two peaks of the ground-state wave function merge into a single distribution centered at the origin. From these qualitative considerations one expects the approximate wave function (4) to work best for large values of λ^2—in particular, for values of λ^2 such that the particle no longer "feels" the hump in the double-well potential. This will occur for $\langle x^4 \rangle \gg \langle x^2 \rangle$. Using $\langle x^4 \rangle = 3\langle x^2 \rangle^2$, $\langle x^2 \rangle = 1/(2g)$, and $g \sim (24/\lambda^2)^{1/3}$ for large λ^2, the criterion for the approximation (4) to be valid takes the form

$$\lambda^2 \gg \tfrac{64}{9} \sim 7 . \tag{7}$$

The regime defined by the inequality (7) will be termed the "displacive" regime, since the ground-state wave function of the system closely resembles that of a simple oscillator. If now the magnitude of λ^2 is reduced in value until the particle zero-point energy becomes comparable to the depth of one of the potential minima ($\lambda^2 \sim 0.2$), a regime is entered in which the wave function no longer resembles an oscillator state, but rather is characteristic of a particle tunneling between the potential barrier separating the two minima of the potential

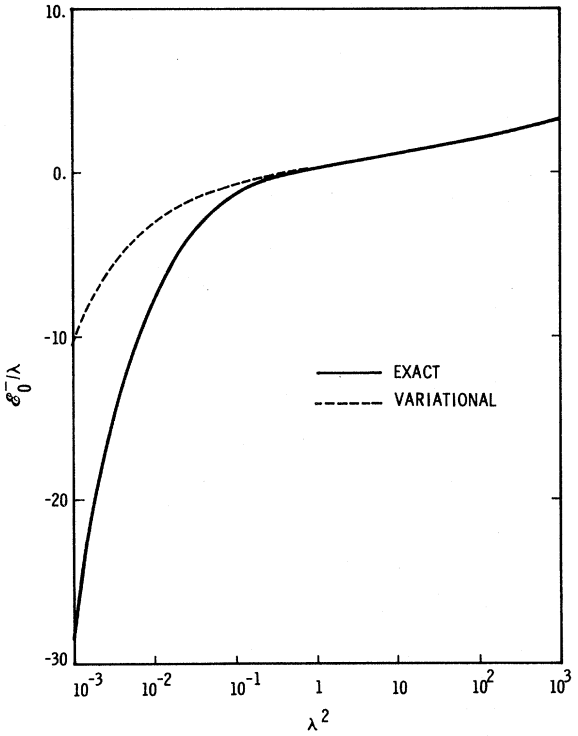

FIG. 2. Plot of the ground-state energy vs λ^2 as obtained from the exact and variational treatments of $H_0^-(u)$.

well—this is the so-called "order-disorder" regime.

The above considerations can serve as a guide in establishing approximations valid in the large- and small-λ^2 regimes, with the exact solution providing a bridge between these two limits. We have already discussed in some detail the approximation based on the variational wave function (4) and have suggested that it should provide a good description of the displacive regime. Indeed, this is the case as can be seen from Figs. 2 and 3 where the ground-state energy $\mathcal{E}_0^-$ and excitation energy $\mathcal{E}_1^- - \mathcal{E}_0^-$ are plotted as functions of λ^2. The solid curves represent the exact solutions obtained from the accurate numerical diagonalization of H_0^-, while the dashed curves are derived from the approximation (4). Figure 2 illustrates the quite remarkable agreement between the exact and approximate ground-state energy for all $\lambda^2 \gtrsim 1$. The excitation energy $\mathcal{E}_1^- - \mathcal{E}_0^-$ is a much more sensitive test of the approximation and, as can be seen from Fig. 3, significant deviations between the approximate and true curves begin to appear at $\lambda^2 \sim 10$. Below this value of λ^2 the approximation becomes increasingly poor. Indeed, the self-consistent choice for $(\mathcal{E}_1^- - \mathcal{E}_0^-)/\lambda^2$ is simply g, and this can be seen from (6) to approach a constant value of 3 for small λ^2, whereas the exact $(\mathcal{E}_1^- - \mathcal{E}_0^-)/\lambda^2$ approaches zero as $\lambda^2 \to 0$.

In the order-disorder limit a seemingly good description would be to choose approximate ground- and first-excited-state wave functions Ψ_0 and Ψ_1 as symmetric and antisymmetric combinations, respectively, of displaced-oscillator states. That is, we choose the states Ψ_0 and Ψ_1 to have the form (apart from normalization)

$$\begin{pmatrix}\Psi_0\\ \Psi_1\end{pmatrix} = \Psi_L \pm \Psi_R\,, \tag{8a}$$

where

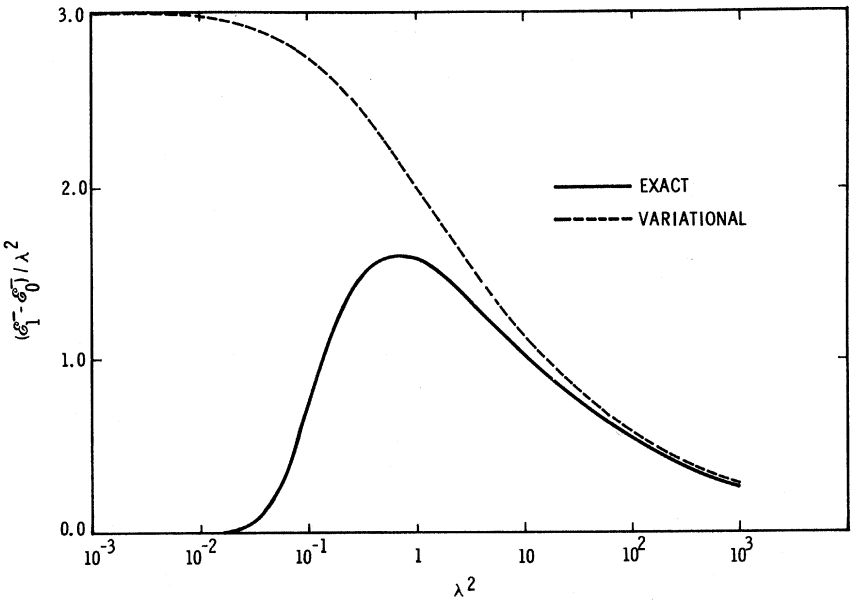

FIG. 3. Plot of the excitation energy vs λ^2 as obtained from the exact and variational treatments of $H_0^-(u)$.

$$\begin{pmatrix}\Psi_L\\ \Psi_R\end{pmatrix}=\left(\frac{g}{\pi}\right)^{1/4}e^{-g(u\pm u_0)^2/2}. \tag{8b}$$

The parameters g and u_0 are chosen so as to minimize the energy of one of the displaced-oscillator states,[26] i.e.,

$$\frac{\partial\langle\Psi_R|H_0^-|\Psi_R\rangle}{\partial g}=\frac{\partial\langle\Psi_L|H_0^-|\Psi_L\rangle}{\partial u_0}=0,$$

where

$$\langle\Psi_R|H_0^-|\Psi_R\rangle=\langle\Psi_L|H_0^-|\Psi_L\rangle$$
$$=\tfrac{1}{4}\lambda^2 g-2/g+3/g^2+(12/g)u_0^2-4u_0^2+4u_0^4. \tag{9}$$

The optimum values of g and u_0 are then obtained as solutions of the coupled equations

$$u_0^2=\tfrac{1}{2}(1-3/g)$$

and (10)

$$\lambda^2 g^3=24+48u_0^2 g-8g.$$

The approximate ground-state energy computed in this way agrees remarkably well ($\lesssim 0.1\%$) with the exact ground-state energy for all $\lambda^2\lesssim 0.1$. Again, however, the excitation energy is the most sensitive test of the approximation. Thus, we use the approximate wave functions (8) to compute

$$\frac{\langle\Psi_1|H_0^-|\Psi_1\rangle}{\langle\Psi_1|\Psi_1\rangle}-\frac{\langle\Psi_0|H_0^-|\Psi_0\rangle}{\langle\Psi_0|\Psi_0\rangle}=\frac{\frac{3}{8}u_0^2\lambda^2 g^2}{\sinh(gu_0^2)}. \tag{11}$$

A calculation of the excitation energy as a function of λ^2 using (11) yields the dashed curve of Fig. 4. This is to be compared with the exact excitation energy which is plotted as the solid curve in the same figure. It is clear that the approximate excitation energy can differ from the exact energy by as much as several orders of magnitude. Thus, the approximation just considered, although providing an adequate evaluation of $\mathcal{E}_0^-$, is not satisfactory for calculating the excitation energy. This shortcoming can be traced to the fact that the approximate ground-state wave function (8) underestimates the overlap in the region near $u=0$. This is illustrated in Fig. 5 where the approximate and exact ground-state wave functions are plotted for $\lambda^2=0.04$. It is clear that (8) mirrors the form of the exact wave function extremely well except in the region near $u=0$, where the dominant contribution to the excitation energy is found. Thus, an approximation of the type (8) does not provide a reliable guide to the magnitude of the tunneling frequency in the order-disorder regime. Improvements to this approximation are being pursued and will be discussed in a later publication.

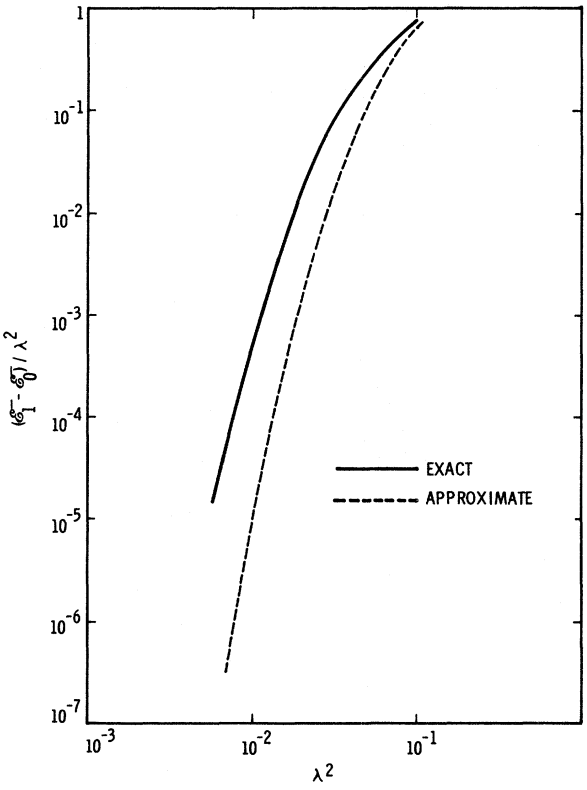

FIG. 4. Comparison of the exact excitation energy of $H_0^-(u)$ as a function of λ^2 with the excitation energy obtained from an approximation in which the ground- and first-excited-state wave functions are taken as symmetric and antisymmetric combinations of off-center Gaussians.

So far little mention has been made of the case where the particle moves in an anharmonic, but single-well, potential. We have already seen that the use of the undisplaced-oscillator wave function (4) provides a good description of the ground-state and excitation energies of $H_0^-(u)$ in the large-λ^2 regime where the particle no longer feels the hump in the double well. It is thus to be expected that for the anharmonic single-well potential the variational approximation should work quite well over the entire range of λ^2 values. In Fig. 6, $\mathcal{E}_0^+$ and $\mathcal{E}_1^+-\mathcal{E}_0^+$ derived from the exact and variational treatments of $H_0^+(u)$ are plotted as functions of λ^2. As anticipated, the low-lying energy spectrum of the single-well quartic oscillator is reproduced almost exactly by the variational approximation. This lends strong support to the validity of the "self-consistent-phonon-approximation" (SPA) treatment of the vibrational properties of crystals in which the dominant contribution to the anharmonicity arises from the quartic interaction.[27] If the harmonic-force matrix is not positive definite, one expects the SPA to be best at high temperatures—in particular, at temperatures for which the thermal energy $k_B T$ exceeds the depth of one of the minima of the effective double-well associated with the unstable normal mode. On the other hand, if the lattice is intrinsically stable, with the harmonic

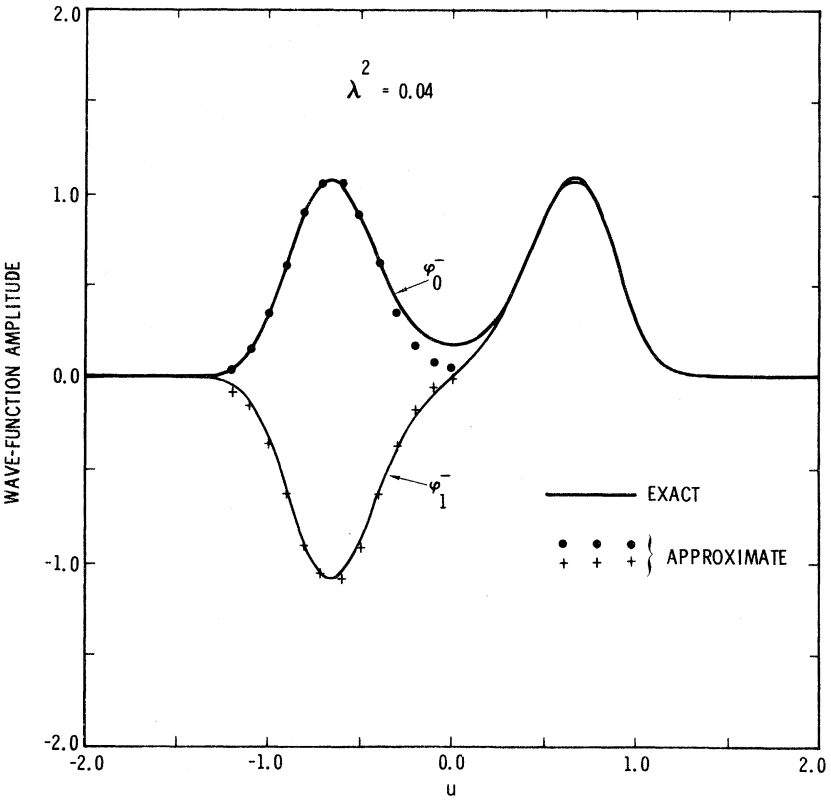

FIG. 5. Comparison of the true ground- and first-excited-state wave functions at $\lambda^2 = 0.04$ with the wave functions obtained from the approximation of Fig. 4.

force matrix positive definite, then the self-consistent phonon approximation is expected to work well over a wide range of temperature. A further discussion of the analogy between the present calculation and the SPA will be deferred to Sec. V of this paper. There we will consider in more detail

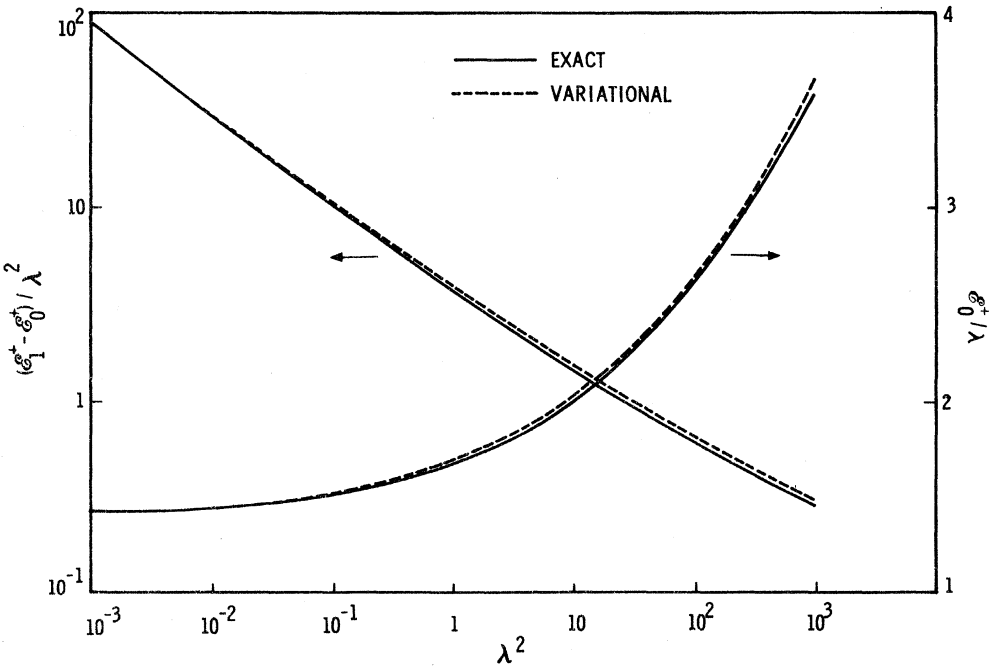

FIG. 6. Plots of the ground-state and excitation energy vs λ^2 as obtained from the exact and variational treatments of $H_0^+(u)$.

the correspondence which exists between λ and an effective temperature.

III. TRANSITION IN SYSTEM OF COUPLED OSCILLATORS

A. Different Physical Systems

It is to be noted that the original model Hamiltonian (1) is an even function of the particle displacements, whereas a mean-field treatment of the bilinear interaction introduces a term linear in the particle displacement. Thus, although the diagonal matrix element of the position variable u in any of the eigenstates of the Hamiltonian (1) is identically zero, it is possible in the presence of the symmetry-breaking field that at some λ_c^2 it will become energetically favorable for the particle to make a transition to a state in which $\langle u \rangle$ is nonzero. Such is the situation described by the effective Hamiltonians (3). We will be distinguishing between an "instability-driven" transition, described by $H^-(u)$, and a "field-driven" transition, described by $H^+(u)$. In the former case the system is intrinsically unstable and one expects a transition to occur for any positive value of the coupling strength χ. In the latter case, however, where the lattice is intrinsically stable, it is expected that a critical value of the coupling strength must be exceeded before the lattice undergoes a transition. The eigenvalue and eigenfunction spectrum associated with the exact treatment of $H^{\pm}(u)$ will be denoted by $\tilde{\mathcal{E}}_n^{\pm}$ and $\tilde{\varphi}_n^{\pm}$, respectively.

In Secs. III B–III D we consider the details of treating the Hamiltonians H^+ and H^- both approximately and exactly. Table I summarizes the predicted transition character yielded by the exact and the approximate treatments.

B. Instability-Driven Case–Exact vs "Two-Level" Treatment

As a prelude to a determination of the self-consistent solutions of the Hamiltonian $H^-(u)$, we consider the somewhat simpler problem of examining the eigenfunction and eigenvalue spectrum of $H_0^-(u) - Fu$ as a function of λ^2 and an externally applied field F. In the region of λ^2 for which the true ground-state wave function of $H_0^-(u)$ describes the particle as being well localized in one of the other of the wells of the double-minima potential, one expects the energies of the two lowest-lying states of $H_0^-(u)$ to be well separated from the energies of the higher excited states. Thus, if the field F is small enough so as not to induce transitions to the higher-lying states, one can as a first approximation diagonalize the full Hamiltonian $H_0^-(u) - Fu$ in the 2×2 subspace defined by φ_0^- and φ_1^-, the ground and first-excited states, respectively, of $H_0^-(u)$. Figure 7 depicts the λ dependence of the ratio of the excitation energy of the second-excited state to that of the first-excited state and it would appear from the plot that the two-level approximation should work best in the region where $\lambda^2 \lesssim 0.10$. The numerical diagonalization of the Hamiltonian $H_0^-(u)$ as a function of λ^2 provides all the information necessary for determining the complete properties of the transition in the two-level approximation. Thus, if

$$H_0^- \begin{pmatrix} \varphi_0^- \\ \varphi_1^- \end{pmatrix} = \begin{pmatrix} \mathcal{E}_0^- \varphi_0^- \\ \mathcal{E}_1^- \varphi_1^- \end{pmatrix},$$

then

$$(H_0^- - Fu) \begin{pmatrix} \tilde{\varphi}_0^- \\ \tilde{\varphi}_1^- \end{pmatrix} = \begin{pmatrix} \tilde{\mathcal{E}}_0^- \tilde{\varphi}_0^- \\ \tilde{\mathcal{E}}_1^- \tilde{\varphi}_1^- \end{pmatrix}. \tag{12}$$

The new energies and wave functions are then given in the two-level approximation by

$$\begin{aligned} \begin{pmatrix} \tilde{\mathcal{E}}_0^- \\ \tilde{\mathcal{E}}_1^- \end{pmatrix} &\cong \tfrac{1}{2}\{\mathcal{E}_0^- + \mathcal{E}_1^- \mp [(\mathcal{E}_1^- - \mathcal{E}_0^-)^2 + 4F^2d^2]^{1/2}\}, \\ \begin{pmatrix} \tilde{\varphi}_0^- \\ \tilde{\varphi}_1^- \end{pmatrix} &\cong \frac{1}{(1+v^2)^{1/2}} \begin{pmatrix} -v\varphi_0^- + \varphi_1^- \\ \varphi_0^- + v\varphi_1^- \end{pmatrix}, \end{aligned} \tag{13}$$

where

$$d = \langle \varphi_0^- | u | \varphi_1^- \rangle$$

and

$$v = \frac{2Fd}{\mathcal{E}_1^- - \mathcal{E}_0^- - [(\mathcal{E}_1^- - \mathcal{E}_0^-)^2 + 4F^2d^2]^{1/2}}.$$

The ground-state average of the particle displacement as a function of field is given by

$$\langle \tilde{\varphi}_0^- | u | \tilde{\varphi}_0^- \rangle \equiv \langle u \rangle = \frac{2Fd^2}{[(\mathcal{E}_1^- - \mathcal{E}_0^-)^2 + 4F^2d^2]^{1/2}}. \tag{14}$$

In Fig. 8 we depict the manner in which the ground-state wave function $\tilde{\varphi}_0$ evolves in the presence of the field F. In the small-λ^2 regime the major effect of the field on the symmetric combination of off-center Gaussian-like structures is that of diminishing the amplitude of one peak relative to the other. On the other hand, for larger values of λ^2 the effect of the field is to shift the entire central distribution to one side.

If we insert into (14) the mean field $F = \chi\langle u \rangle$, we obtain the self-consistent displacement as the solu-

TABLE I. Values of the coupling strength χ for which transitions of a particular character are found in the exact, variational, and two-level treatments of the instability-driven (ID) and field-driven (FD) systems.

Character of transition	Exact	Variational	Two-level
No transition	$\chi = 0$ (ID) $0 < \chi \leq 8$ (FD)	$0 < \chi \leq 8$ (FD)	$\chi = 0$ (ID)
First order		$\chi \geq 0$ (ID)	
Second order	$\chi > 0$ (ID) $\chi > 8$ (FD)	$\chi > 8$ (FD)	$\chi > 0$ (ID)

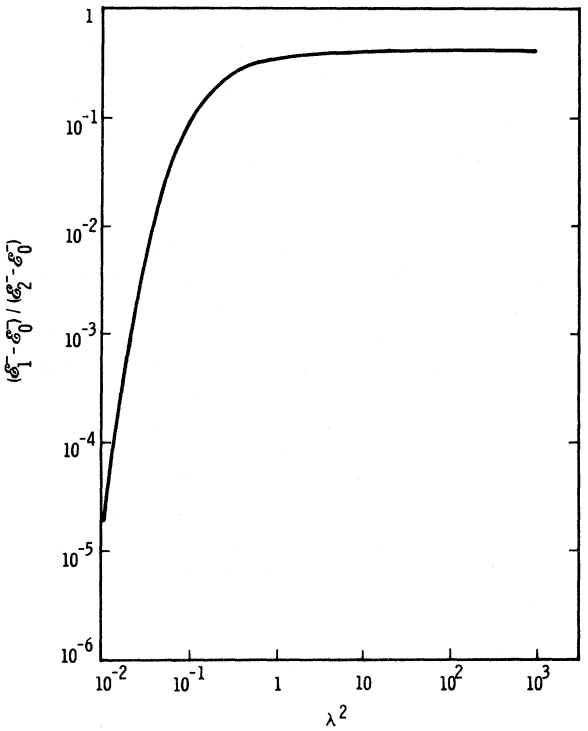

FIG. 7. Plot of the ratio of the two lowest-lying excitation energies of $H_0^-(u)$ as a function of λ^2.

tion to the equation

$$\langle u\rangle = \frac{2\chi\langle u\rangle d^2}{[(\mathcal{E}_1^- - \mathcal{E}_0^-)^2 + 4\chi^2\langle u\rangle^2 d^2]^{1/2}} . \tag{15}$$

Equation (15) yields two possible solutions: the obvious solution $\langle u\rangle = 0$ together with the displaced solution

$$\langle u\rangle^2 = d^2 - (\mathcal{E}_1^- - \mathcal{E}_0^-)^2/(4\chi^2 d^2). \tag{16}$$

For $d < (\mathcal{E}_1^- - \mathcal{E}_0^-)/(2\chi d)$ the minimum energy occurs for $\langle u\rangle = 0$ and is simply $\mathcal{E}_0^-$. For $d > (\mathcal{E}_1^- - \mathcal{E}_0^-)/(2\chi d)$, however, the minimum energy occurs for a nonzero value of $\langle u\rangle$ and is given by

$$\tilde{\mathcal{E}}_0^- = \tfrac{1}{2}\{\mathcal{E}_1^- + \mathcal{E}_0^- - [(\mathcal{E}_1^- - \mathcal{E}_0^-)^2 + 4\chi^2 d^2\langle u\rangle^2]^{1/2}\}$$
$$= \tfrac{1}{2}(\mathcal{E}_1^- + \mathcal{E}_0^- - 2\chi d^2) . \tag{17}$$

A transition from one state to the other is signaled by the vanishing of the expression (16). Since $(\mathcal{E}_1^- - \mathcal{E}_0^-)$ is a rapidly increasing function of λ^2, with d remaining relatively constant, the critical value λ_c at which the transition occurs is an increasing function of the coupling strength χ. Furthermore, one can expand d and $(\mathcal{E}_1^- - \mathcal{E}_0^-)$ in powers of λ^2 about the point λ_c^2 to obtain

$$\langle u\rangle^2 \propto (\lambda_c^2 - \lambda^2) \propto 2\lambda_c(\lambda_c - \lambda)$$

or

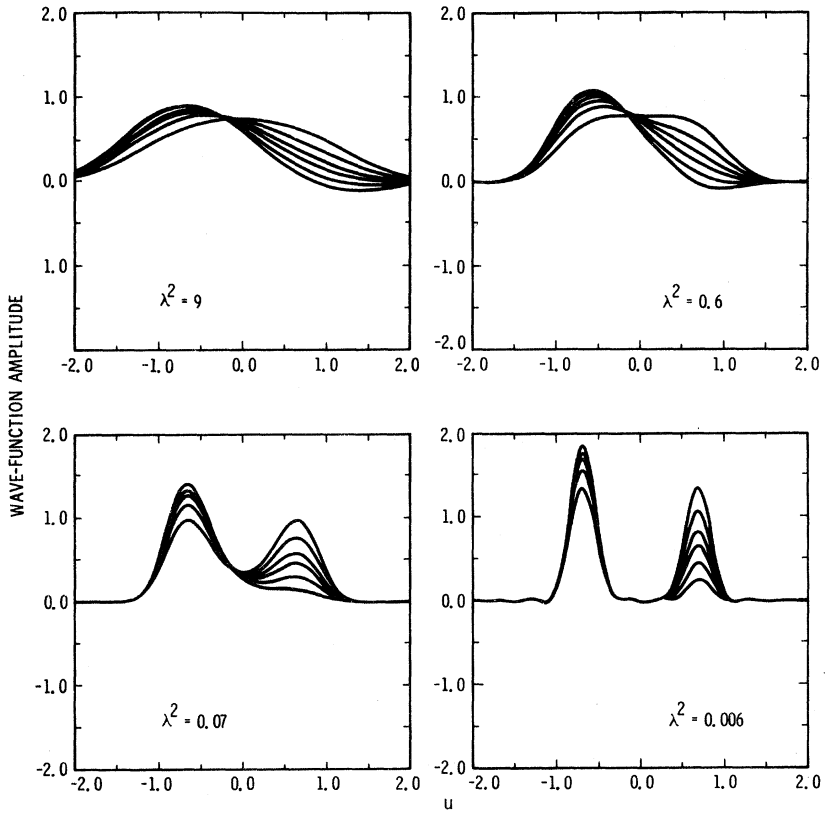

FIG. 8. Plot of the way in which the ground-state wave function of the two-level approximation evolves in the presence of a symmetry-breaking field in the various λ^2 regimes. The various curves correspond to different values of the applied field.

$$\langle u\rangle \propto (\lambda_c - \lambda)^{1/2}, \tag{18}$$

which is the usual molecular-field result if we identify λ with temperature. The square-root behavior of the order parameter $\langle u\rangle$ as a function of λ in the vicinity of the transition is not just an artifact of the two-level approximation. Indeed, as we show in the Appendix, the exact solution of the Hamiltonian (2) also yields the result (18). In the limit $\lambda \to 0$ the ground state of $H_0^-(u)$ becomes doubly degenerate with wave functions represented by symmetric and antisymmetric combinations of δ functions centered at the minima of the double-well potential. Thus, as $\lambda \to 0$, $d \to 1/\sqrt{2}$, $(\mathcal{E}_1^- - \mathcal{E}_0^-) \to 0$, and $\langle u\rangle$ saturates at the value $1/\sqrt{2}$.

Figure 9 depicts the behavior of the self-consistent displacement squared as a function of λ for increasing values of the coupling strength χ, with results from both the exact solution and the two-level approximation being illustrated. The solid lines representing the exact solution were obtained from a numerical diagonalization of the full Hamiltonian $H_0^-(u) - Fu$, subject to the self-consistency condition $F = \chi\langle\tilde{\varphi}_0^-|u|\tilde{\varphi}_0^-\rangle$. It is easily seen (see the Appendix) that, if the transition of the exact treatment is second order, it occurs when

$$\left(\frac{\delta\langle\tilde{\varphi}_0^-|u|\tilde{\varphi}_0^-\rangle}{\delta F}\right)_{F=0} = \chi^{-1}. \tag{19}$$

It is to be noted that the two-level approximation predicts a $\lambda = 0$ saturation value for $\langle u\rangle^2$ equal to $\frac{1}{2}$, irrespective of the magnitude of the coupling strength. On the other hand, elementary stability arguments tell us that in the presence of the self-consistent field the true saturation value of $\langle u\rangle^2$ should be $\frac{1}{2}(1 + \frac{1}{8}\chi)$, as exhibited by the solid curves in Fig. 9. For values of the coupling strength greater than 0.05 the agreement between the exact treatment and the two-level approximation in the region $\lambda < \lambda_c$ becomes increasingly

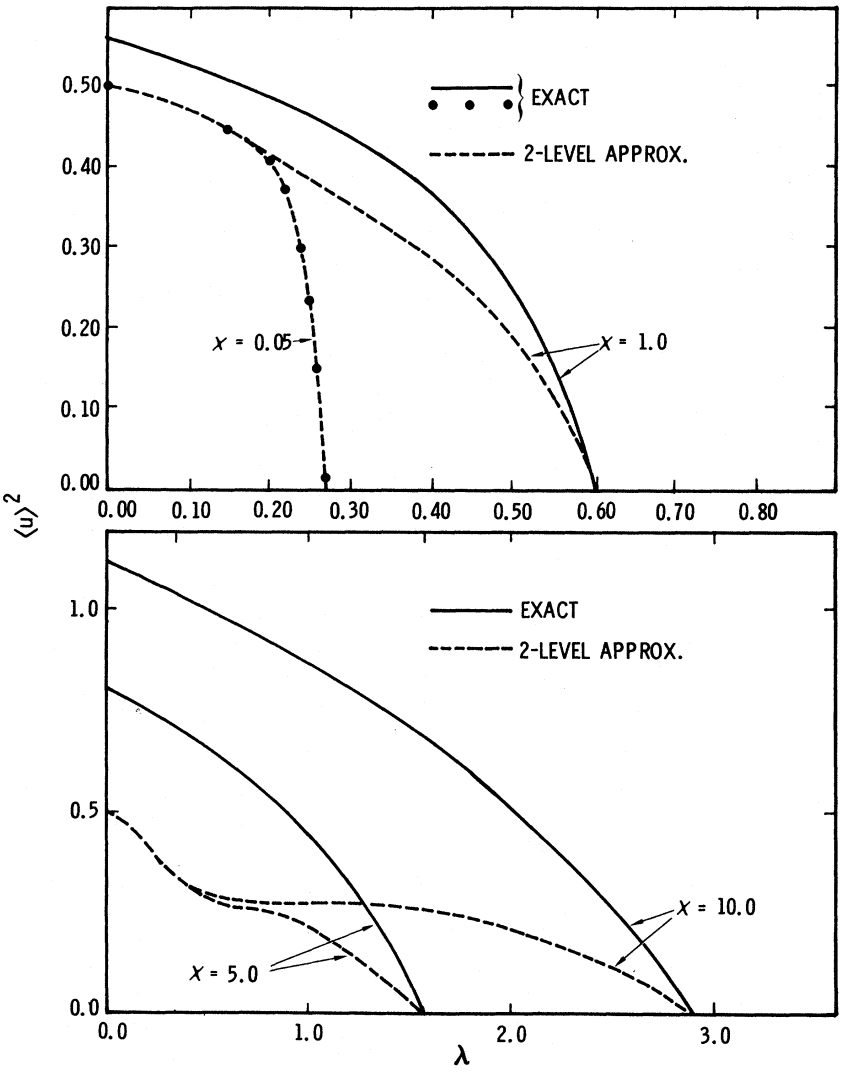

FIG. 9. Plots of the square of the order parameter $\langle u\rangle$ vs λ for the exact and two-level approximation treatments of the instability-driven transition.

worse. Nonetheless, this approximate treatment provides a reasonably accurate evaluation of λ_c, the critical λ value at which the transition occurs. The reasons for the success of the two-level approximation in determining λ_c will be discussed in Sec. V.

A striking feature of the plot in Fig. 9 is the fact that the transition becomes increasingly sharp as λ_c decreases. Indeed, for $\chi \leq 0.05$ the transition is almost first order in character, reflecting the underlying intrinsic instability imposed on the system by the double-minima potential field. For λ_c in the small-λ regime the rapid increase of the order parameter below the transition point is a characteristic feature of the instability-driven transition.

C. Instability-Driven Case—Exact vs Variational Treatment

The above considerations were carried out within the context of a comparison of the exact treatment of the instability-driven transition with the two-level approximation. It is instructive at this point to consider yet a further approximation—an approximation motivated in part by the success of the trial oscillator wave function (4) in describing the low-lying excitation spectrum of $H_0^-(u)$ in the large-λ^2 regime (see Figs. 2 and 3). This suggests that we attempt to describe the transition through the introduction of a displaced-oscillator function of the form (8b) as an approximation for the true ground-state wave function in the presence of the symmetry-breaking field. Computing the expectation value of the Hamiltonian $H_0^-(u) - Fu$ with respect to the function (8b) yields an expression for the energy identical to (9), but with the addition of a term $(-Fu_0)$. A subsequent minimization of the energy with respect to u_0 and g results in the following two coupled equations:

$$\begin{aligned} &16u_0^3 + 8(3/g - 1)u_0 = F, \\ &\lambda^2 g^3 + 8g - 48gu_0^2 - 24 = 0. \end{aligned} \tag{20}$$

Inserting now the self-consistent value χu_0 for the field F yields one set of equations for the undisplaced state:

$$\begin{aligned} &u_0 = 0, \\ &\lambda^2 g^3 + 8g - 24 = 0, \end{aligned} \tag{21a}$$

and an additional independent set for the displaced state:

$$\begin{aligned} &u_0^2 = \tfrac{1}{16}(8 - 24/g + \chi), \\ &\lambda^2 g^3 - (3\chi + 16)g + 48 = 0. \end{aligned} \tag{21b}$$

Equation (21a) gives rise to three solutions for g, only one of which is real. This latter solution is positive for all $\lambda \geq 0$ and can be shown to represent at least a local minimum of E_0 for $\lambda > \lambda_1 = \frac{1}{24}\chi^{1/2}(\chi + 8)$ and a local maximum for $\lambda < \lambda_1$. Furthermore, it possesses the following limiting properties:

$$\begin{aligned} &g \to 3, \quad \lambda \to 0 \\ &g = 24/(\chi + 8), \quad \lambda = \lambda_1, \\ &g \to (24/\lambda^2)^{1/3}, \quad \lambda \to \infty. \end{aligned} \tag{22}$$

A consideration of Eq. (21b) describing the displaced state indicates that there exists a limiting $\lambda_2 = \frac{1}{24}(\chi + \frac{16}{3})^{3/2}$ above which no real and positive displaced solutions are possible, but below which two such solutions exist. If we label these solutions g_1 and g_2, then they exhibit the limiting properties

$$\begin{aligned} &g_1 = g_2 = 24/(\chi + \tfrac{16}{3}), \quad \lambda = \lambda_2 \\ &\left.\begin{aligned} g_1 &\sim (3\chi + 16)^{1/2}/\chi \\ g_2 &\sim 16/(\chi + \tfrac{16}{3}) \end{aligned}\right\} \quad \lambda \to 0. \end{aligned} \tag{23}$$

Furthermore, the self-consistent displacement corresponding to the solution g_1 satisfies

$$\tfrac{1}{2}(1 + \tfrac{1}{8}\chi) \leq u_0^2 \leq \tfrac{1}{6}, \quad 0 \leq \lambda \leq \lambda_2 \tag{24}$$

whereas the self-consistent displacement associated with g_2 satisfies

$$-\tfrac{1}{32}\chi \leq u_0^2 \leq \tfrac{1}{6}, \quad 0 \leq \lambda \leq \lambda_2.$$

For the solution g_1, the displacement u_0 increases with decreasing λ, saturating at the value $[\frac{1}{2}(1 + \frac{1}{8}\chi]^{1/2}$—this is the physical solution. It corresponds to at least a local minimum of the energy in the interval $0 \leq \lambda \leq \lambda_2$. The solution g_2, however, corresponds to having u_0 *decrease* with decreasing λ, passing through zero at $\lambda = \lambda_1$ and then becoming imaginary—this is the unphysical solution. It corresponds to a local maximum of the free energy. In general, the energies associated with the undisplaced and displaced solutions cross at some λ_c in the interval $\lambda_1 < \lambda < \lambda_2$ with the transition between the two states being distinctly first order.

In Fig. 10 we plot the λ dependence of the squared order parameter associated with both the physical and unphysical displaced solutions for a series of increasing χ values. λ_1, the lower limit of metastability for the undisplaced solution, has been denoted the "supercooling point" while λ_2, the upper limit of metastability for the displaced solution, has been denoted the "superheating point." λ_1, λ_c, and λ_2 all approach the asymptotic value $\frac{1}{24}\chi^{3/2}$ for large χ with the transition becoming more second order in character. We should note that the variational treatment predicts a transition for $\chi = 0$. In this case $\lambda = 0$ is the supercooling point. As will be discussed in the Sec. V, the first-order transition which occurs for the case of zero-coupling strength is actually due to the restricted form of the variational wave function,

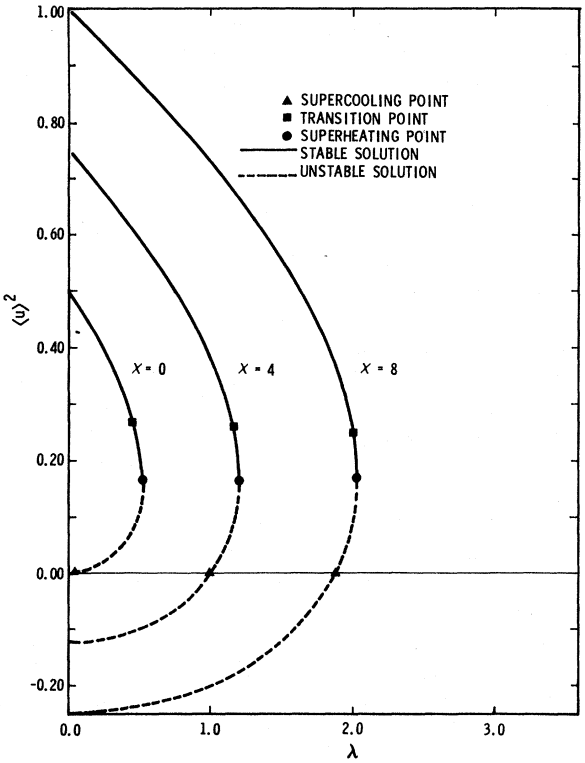

FIG. 10. λ dependence of the squared order parameter $\langle u\rangle^2$ associated with the stable and unstable solutions obtained from the variational treatment of the instability-driven transition.

since the exact treatment predicts no transition for $\chi = 0$.

Figure 11 compares some of the predictions of the variational calculation with those of the exact calculation for increasing values of the coupling strength. In both cases the transition point increases with increasing χ. However, as we pointed out above, the first-order transition point of the variational treatment approaches a nonvanishing value, whereas the λ_c associated with the exact solution approaches zero as $\chi \to 0$. We note that for small values of the coupling strength, the actual second-order transition occurs well beyond the supercooling point but below the superheating point, whereas for larger values of χ the actual transition occurs beyond both metastability points. The relation between the metastability points of the variational treatment and the actual second-order transition point will be discussed in more detail later.

For the instability-driven transitions which occur at large χ values, the zero-point energy of the particle will considerably exceed the depth of the potential minima. In such a situation the particle primarily feels the quartic contribution from the potential field. Thus, it seems reasonable that for transitions occurring for large values of the coupling strength the qualitative features of the transition in the immediate vicinity of the transition point should be similar in both the instability- and field-driven cases. We will examine this point in more detail in Sec. III D.

D. Field-Driven Case—Exact vs Variational Treatment

As we emphasized in relation to Fig. 6, the variational-oscillator wave function provides an excellent evaluation of the ground-state and low-lying excitation energies of the quartic Hamiltonian $H_0^+(u)$ over the entire range of λ values considered. Thus, it would be expected that such an approximation would provide a qualitatively reasonable description of the field-driven transition. We compute the ground-state expectation value of $H^+(u)$ with respect to one of the displaced oscillator functions (8b), obtaining[28]

$$\langle \Psi_L | H^+(u) | \Psi_L \rangle = \tfrac{1}{4}\lambda^2 g + 2/g + 3/g^2 + (12/g)u_0^2 + 4u_0^2 + 4u_0^4 - \tfrac{1}{2}\chi u_0^2 . \quad (25)$$

The requirement that this energy represents an extremum with respect to u_0 and g yields two independent sets of self-consistent equations:

$$u_0 = 0 ,$$

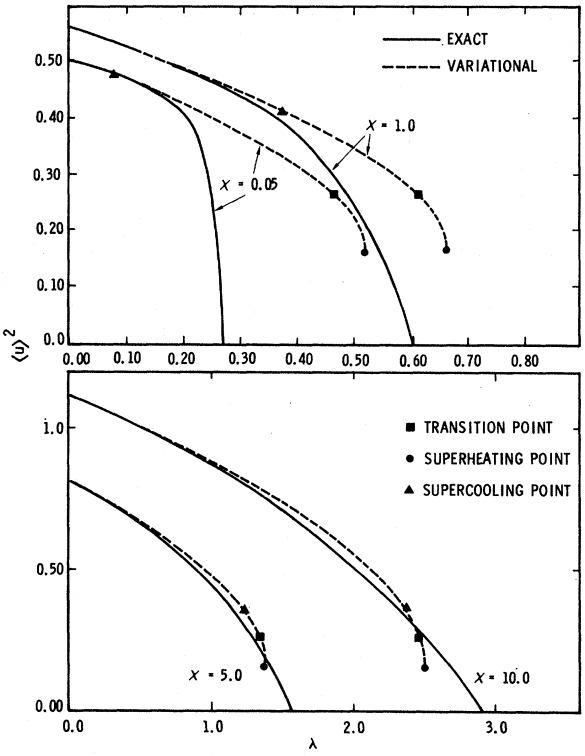

FIG. 11. λ dependence of the squared order parameter $\langle u\rangle^2$ associated with the exact and variational treatments of the instability-driven transition.

$$\lambda^2 g^3 - 8g - 24 = 0; \tag{26a}$$

and

$$u_0^2 = \tfrac{1}{16}(\chi - 8 - 24/g), \quad \lambda^2 g^3 - (3\chi - 16)g + 48 = 0. \tag{26b}$$

In the undisplaced state, Eq. (26a), a positive and real g solution can be found for all values of λ. However, this solution represents a minimum of (25) only if $g < 24/(\chi - 8)$, which is satisfied for $\lambda > \frac{1}{24}\chi^{1/2}(\chi - 8)$. The various limiting values of the undisplaced g solution are given by

$$\begin{aligned} &g \to (24/\lambda^2)^{1/3}, && \lambda \to \infty \\ &g = 24/(\chi - 8), && \lambda = \tfrac{1}{24}\chi^{1/2}(\chi - 8) \\ &g \to 2^{3/2}/\lambda, && \lambda \to 0. \end{aligned} \tag{27}$$

It is clear from the above that we must have $\chi > 8$ in order for the undisplaced g solution to represent a stable solution at large λ.

Equation (26b) governing the displaced state has two positive and real g solutions for $\lambda < \lambda_0 = \frac{1}{12}(\chi - \frac{16}{3})^{3/2}$. Denoting these two solutions by g_1 and g_2, they exhibit the limiting properties

$$\begin{aligned} &g_1 = g_2 = 24/(\chi - \tfrac{16}{3}), && \lambda = \lambda_0 \\ &g_1 \sim (3\chi - 16)^{1/2}/\lambda, \\ &g_2 \sim 48/(3\chi - 16), \end{aligned} \quad \lambda \to 0. \tag{28}$$

The order parameter associated with solution g_1 satisfies

$$\tfrac{1}{16}(\chi - 8) \le u_0^2 \le -\tfrac{1}{6}, \quad 0 \le \lambda \le \lambda_0.$$

This is the physical solution—it gives rise to a vanishing order parameter for $\lambda = \lambda_c = \frac{1}{24}\chi^{1/2}(\chi - 8)$ and the transition between displaced and undisplaced states is second order. We note that the saturation value of u_0^2 at λ_0 is $\frac{1}{16}(\chi - 8)$ so that again we see that one must have $\chi > 8$ in order for a transition to occur at all. The order parameter associated with the unphysical solution satisfies

$$-\tfrac{1}{32}\chi \le u_0^2 \le -\tfrac{1}{6}, \quad 0 \le \lambda \le \lambda_0$$

and is always imaginary.

In Fig. 12 we plot the λ dependence of the squared order parameter associated with the exact and variational treatments of the field-driven transition. It is clear that the variational solution reproduces the behavior of the exact solution extremely well except in the immediate vicinity of the second-order transition point. In general, the λ_c predicted by the approximate treatment lies below the actual λ_c. This last might have been anticipated, since we saw previously that for the instability-driven transitions occurring in the large-λ regime (see Fig. 11) the actual second-order transition point was situated above the transition point of the variational treatment. The relation which determines the point at which the actual second-order transition of the field driven case occurs is given by Eq. (19) with $\tilde{\varphi}_0^-$ replaced by $\tilde{\varphi}_0^+$.

IV. COLLECTIVE PROPERTIES

Central to any discussion of second-order structural transformations in crystals is the so-called "soft mode," i.e., a collective mode of the system whose characteristic energy vanishes at the transition point. The idea of the soft mode was first introduced within the context of displacive ferroelectrics by Cochran[9] and Anderson[8] and has since received considerable attention. From the experimental point of view the soft-mode concept is of great importance, since the anomalous temperature dependence of the mode near the transition can, in many cases, be observed using the techniques of inelastic neutron scattering and light scattering. In displacive ferroelectrics the soft mode is usually identified with a low-lying transverse-optic-phonon frequency, whereas in ferroelectrics of the order-disorder type the soft mode exhibits the characteristics of a tunneling mode or, perhaps, a coupled phonon-tunneling mode.

In Secs. I–III we found that the characteristic low-lying excitation energy associated with the exact and variational treatments of the static molecular field Hamiltonians (3) were $\mathcal{E}_1^{\pm} - \mathcal{E}_0^{\pm}$ and $\lambda^2 g$, respectively. In the instability-driven cases $\mathcal{E}_1^- - \mathcal{E}_0^-$ did not vanish at the second-order transition point of the exact treatment nor did $\lambda^2 g$ vanish at the supercooling point of the variational treatment. Similarly, in the field-driven case, neither $\mathcal{E}_1^+ - \mathcal{E}_0^+$ nor $\lambda^2 g$ vanish at the respective second-order transition points of the exact and approximate treatments. None of this is surprising, of course, since both $\mathcal{E}_1^{\pm} - \mathcal{E}_0^{\pm}$ and $\lambda^2 g$ are energies associated with single-particle-like motion in the individual potential wells, whereas what we would like to evaluate is the energy associated with a mode which involves the correlated motion of all the particles. In order to evaluate this energy we must consider the response of an individual ion displacement when a time-dependent external probe is applied to the system.

We introduce a time-dependent field of the form $-\sum_l \delta F_l(t) u_l$ into Eq. (1). The resultant Hamiltonian may then be used in conjunction with the equation of motion for the density matrix of the system in order to obtain the linear response of the average particle displacement. Within the context of the molecular-field approximation, one expresses the system density matrix (now time-dependent) as a product of single-particle density matrices, each of which is associated with a single lattice cell.[29]

The result for the linear response of the average particle displacement to a time-dependent pertur-

bation $\delta H(t)$ can be written concisely as[30]

$$\delta\langle u_l\rangle(t) = -i\int_{-\infty}^{t} dt'\langle\Phi_0|[u_l(t),\ \delta H(t')]|\Phi_0\rangle, \quad (29)$$

where Φ_0 denotes the ground-state wave function in the absence of δH. In the molecular-field approximation, the perturbation δH has the form

$$\delta H(t) = -\sum_{ll'}\chi(ll')u_l\delta\langle u_{l'}\rangle(t) - \sum_l F_l(t)u_l \quad (30)$$

and the ground-state average in (29) is with respect to a product of single-particle ground-state wave functions based on one of the static molecular-field Hamiltonians of Eq. (3), i.e., $\Phi_0 = \prod_l \tilde{\varphi}_0^{\pm}(u_l)$. In order to case Eq. (29) into a more tractable form, we introduce a set of intermediate states into the commutator and decompose all time- and lattice-dependent quantities into their appropriate frequency- and wave-vector–dependent Fourier components. After some straightforward algebraic manipulation, the q and ω Fourier transform of the response function $\delta\langle u_l\rangle(t)/\delta F_{l'}(t')$ takes the form[31]

$$\delta\langle u_q\rangle(\omega)/\delta F_q(\omega) = \sum_\alpha{}'|\langle\tilde{\varphi}_0^{\pm}|u|\tilde{\varphi}_\alpha^{\pm}\rangle|^2\frac{2(\tilde{\mathcal{E}}_0^{\pm}-\tilde{\mathcal{E}}_\alpha^{\pm})}{\omega^2-(\tilde{\mathcal{E}}_0^{\pm}-\tilde{\mathcal{E}}_\alpha^{\pm})^2}$$
$$\times\left(1-2\chi(q)\sum_\alpha{}'|\langle\tilde{\varphi}_0^{\pm}|u|\tilde{\varphi}_\alpha^{\pm}\rangle|^2\frac{(\tilde{\mathcal{E}}_0^{\pm}-\tilde{\mathcal{E}}_\alpha^{\pm})}{\omega^2-(\tilde{\mathcal{E}}_0^{\pm}-\tilde{\mathcal{E}}_\alpha^{\pm})^2}\right)^{-1}. \quad (31)$$

The frequencies of the collective modes of the system are defined as the positions of the resonances of the response $\delta\langle u_q\rangle(\omega)/\delta F_q(\omega)$. From Eq. (31) we see that the response function exhibits simple poles for those values of the frequency which satisfy

$$2\sum_\alpha{}'|\langle\tilde{\varphi}_0^{\pm}|u|\tilde{\varphi}_\alpha^{\pm}\rangle|^2\frac{(\tilde{\mathcal{E}}_\alpha^{\pm}-\tilde{\mathcal{E}}_0^{\pm})}{(\tilde{\mathcal{E}}_\alpha^{\pm}-\tilde{\mathcal{E}}_0^{\pm})^2-\omega^2} = \chi^{-1}(q). \quad (32)$$

We graphically illustrate the solutions to Eq. (32) in the plot of Fig. 13. It is clear that there exists one low-lying mode together with an infinite number of higher-lying single-particle-like modes. Since $\chi(0) > \chi(q\neq 0)$, the smallest frequency of the lowest-lying branch occurs for $q=0$. For values of λ above the transition point we can replace $\tilde{\mathcal{E}}_\alpha^{\pm}$ by $\mathcal{E}_\alpha^{\pm}$ and $\tilde{\varphi}_\alpha^{\pm}$ by $\varphi_\alpha^{\pm}$. Approaching the transition point from above, we see that the criterion for the lowest-lying-mode frequency to vanish is simply

$$2\sum_\alpha{}'|\langle\varphi_0^{\pm}|u|\varphi_\alpha^{\pm}\rangle|^2/(\mathcal{E}_\alpha^{\pm}-\mathcal{E}_0^{\pm}) = \chi^{-1}. \quad (33)$$

The relation (33) is identical to the relation (19) which determines the second-order transition point. To see this we need only carry out a linear-response calculation using the Hamiltonian $H_0^{\pm}(u) - Fu$. The results of such a calculation may be obtained from (31) by setting $q=\omega=\chi=0$ and replacing $\tilde{\varphi}_\alpha^{\pm}$ and $\tilde{\mathcal{E}}_\alpha^{\pm}$ by $\varphi_\alpha^{\pm}$ and $\mathcal{E}_\alpha^{\pm}$, respectively. Thus,

$$\left(\frac{\delta\langle u\rangle}{\delta F}\right)_{F=0} = 2\sum_\alpha{}'|\langle\varphi_0^{\pm}|u|\varphi_\alpha^{\pm}\rangle|^2/(\mathcal{E}_\alpha^{\pm}-\mathcal{E}_0^{\pm}),$$

which suffices to show that (33) and (19) are identical. Thus, we see that there exists a long-wavelength collective mode of the system whose energy vanishes at the second-order transition point.

So far our attention has been focused on the exact treatment. On the other hand, in the two-level approximation things simplify considerably. In this approximation there exists only a single collective mode with a frequency defined as

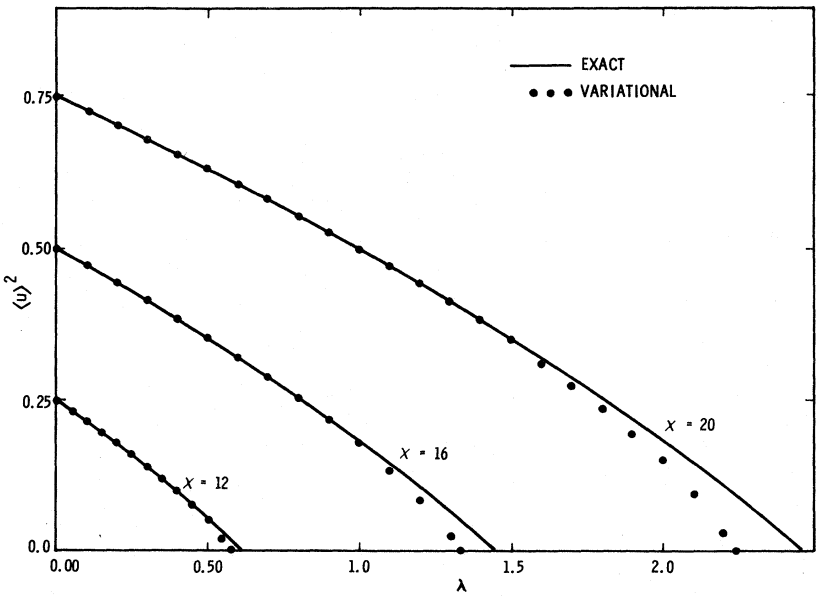

FIG. 12. λ dependence of the squared order parameter $\langle u\rangle^2$ associated with the exact and variational treatments of the field-driven transition.

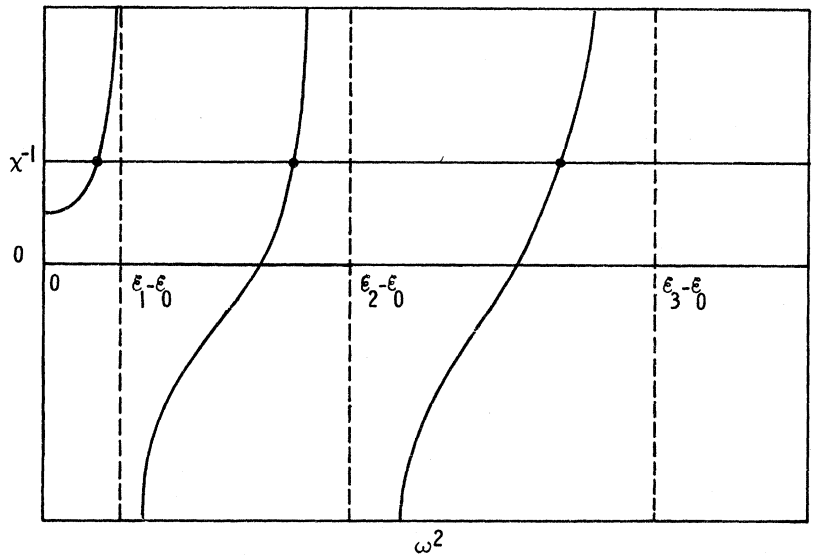

FIG. 13. Plot illustrating the graphical solution of Eq. (32). The solid lines represent the dependence of the left-hand side of Eq. (32) on ω^2. The intersections of the horizontal line with the solid lines yield the positions of the poles of the response function (31).

$$\Omega_q^2 = (\tilde{\mathcal{E}}_1^{\pm} - \tilde{\mathcal{E}}_0^{\pm})^2 - 2\chi(q)\,|\langle\tilde{\varphi}_1^{\pm}|u|\tilde{\varphi}_0^{\pm}\rangle|^2(\tilde{\mathcal{E}}_1^{\pm} - \tilde{\mathcal{E}}_0^{\pm}). \quad (34)$$

The transition in the two-level approximation occurs at the λ value for which expression (16) vanishes. This last is equivalent to Eq. (33) with only the first term in the sum on the left-hand side retained.

As a final exercise prior to concluding this section we evaluate the collective response of the undistorted phase within the framework of the variational approximation employed in Sec. III. We can work directly with Eq. (31). We need only recognize that with $|\varphi_0^{\pm}\rangle$ given by (4), the first-excited state is $\sqrt{2}gu|\varphi_0^{\pm}\rangle$. Thus, the corresponding excitation energy $\mathcal{E}_1^{\pm} - \mathcal{E}_0^{\pm}$ is $\lambda^2 g$, the matrix element $\langle\varphi_0^{\pm}|u|\varphi_1^{\pm}\rangle$ is given by $1/\sqrt{2}g$, and $\langle\varphi_0^{\pm}|u|\varphi_\alpha^{\pm}\rangle = 0$, $\alpha > 1$. Substituting these results into (31), we immediately obtain

$$\frac{\delta\langle u_q\rangle(\omega)}{\delta F_q(\omega)} = \frac{-\lambda^2}{\omega^2 - \lambda^4 g^2 + \lambda^2\chi(q)}\ , \quad (35)$$

and we see that the response has a simple pole at

$$\omega_q^2 = \lambda^2(\lambda^2 g - \chi(q)). \quad (36)$$

In the field-driven case ω_0^2 vanishes at the second-order transition point, whereas in the instability-driven case this squared frequency vanishes at the supercooling point.

V. CONCLUSION

As was noted in Sec. III, the two-level approximation works remarkably well for determining λ_c. The explanation of this becomes apparent if one examines (33) or its equivalent (A24). In the two-level approximation, the summation on the right-hand side of (33) is replaced by a single term so that λ_c is determined by the approximate expression

$$\chi^{-1} = 2\,\frac{\langle\varphi_1^{\pm}(\lambda)|u|\varphi_0^{\pm}(\lambda)\rangle^2}{\mathcal{E}_1(\lambda) - \mathcal{E}_0(\lambda)}\bigg|_{\lambda=\lambda_c}. \quad (37)$$

This expression can also be viewed as the two-level approximation for the vanishing of the response frequency [see Eq. (34)]. We will see that this happens to be a very good approximation.

In the case of H^+ or H^- with χ large, the displacive regime, the transition occurs in a region where the lowest states of $H_0^{\pm}$ are well represented by harmonic-oscillator wave functions. For such wave functions, $|1\rangle \propto u|0\rangle$ and the orthogonality of the states requires that $\langle\alpha|u|0\rangle = 0$, $\alpha \neq 1$. For the states of $H_0^{\pm}$ in the large-χ regime, the approximation $\langle\varphi_\alpha^{\pm}|u|\varphi_0^{\pm}\rangle \ll \langle\varphi_1^{\pm}|u|\varphi_0^{\pm}\rangle$, $\alpha \neq 1$, holds. The large-α states are less well represented by harmonic-oscillator states, but they must still be orthogonal to the true $\alpha = 1$ state which is well represented by $u|\varphi_0^{\pm}\rangle$. The contribution from $\alpha > 1$ terms in (33) is also diminished by the energy denominators, but the orthogonality relations are still the primary effect.

The case of H^- with χ small is the situation for which the two-level approximation was originally devised. Then $\mathcal{E}_1^- - \mathcal{E}_0^- \ll \mathcal{E}_\alpha^- - \mathcal{E}_0^-$, $\alpha > 1$. In addition, $|\varphi_1^-\rangle \approx u|\varphi_0^-\rangle$ is still a good approximation and the orthogonality considerations remain valid.

On the basis of the above, we can confidently make the statement that the two-level approximation always determines λ_c to good accuracy for the system considered in this paper. Unfortunately, this conclusion may not always be useful, because its application requires an exact determination of $\langle\varphi_1^{\pm}|u|\varphi_0^{\pm}\rangle$ and $\mathcal{E}_1^{\pm} - \mathcal{E}_0^{\pm}$. When these quantities cannot be determined exactly, the correct prediction of λ_c requires their accurate approximate evaluation.

Given the fact that λ_c can be reliably predicted from (37), we are now in a position to understand the errors in its determination by the various treatments discussed in Sec. III. There are really two approaches which could be discussed: the way the prediction of λ_c could have been made and the way it actually was determined.

The approach that could have been followed is the simplest case to consider and so will be discussed first. This approach was described at the end of Sec. IV where values were given for $\mathcal{E}_1^+ - \mathcal{E}_0^+$ and $\langle \varphi_1^+ | u | \varphi_0^+ \rangle$ as estimated by the undisplaced-oscillator variational calculation. These results can then be substituted in (37) and the simple result

$$\chi = \lambda^2 g^2(\lambda_c) \tag{38}$$

is obtained with the aid of (21a), (21b), (26a), and (26b).

In the displacive regime, we would expect that $\mathcal{E}_1^+ - \mathcal{E}_0^+$ and $\langle \varphi_1^+ | u | \varphi_0^+ \rangle$ would be estimated reasonably accurately. Because it is a variational calculation, E_0^+ is an upper bound on the true ground-state energy. From symmetry, E_1^+ is also an upper bound on the true energy of the first excited state (the lowest-lying antisymmetric state), since it is the expectation value of H_0^+ with respect to $u|\varphi_0^+\rangle$. However, g is determined so as to minimize E_0^+ and no attempt is made to minimize E_1^+. So we expect that E_0^+ is closer to $\mathcal{E}_0^+$ than is E_1^+ to $\mathcal{E}_1^+$. Therefore, we expect $\langle 1|u|0\rangle \sim \langle \varphi_1^+ | u | \varphi_0^+ \rangle$, but $(E_1^+ - E_0^+) > (\mathcal{E}_1^+ - \mathcal{E}_0^+)$. The validity of this inequality can be established from the graphs of Figs. 3 and 6. This would make the predicted value of λ_c too low. In the order-disorder regime, we see from Fig. 3 that $E_1^- - E_0^-$ is again too large, but by quite a bit. Thus we would expect that the predicted λ_c would be quite a bit too low.

The above is directly related to the calculation that was actually performed in which the ground-state energy was estimated by two different variational wave functions as $E_0^+(u_0 = 0)$ or $E_0^+(u_0 \neq 0)$. At large enough λ, $E_0^+(u_0 = 0) > E_0^+(u_0 \neq 0)$. The transition occurs when $E_0^+(u_0 = 0) = E_0^+(u_0 \neq 0)$. In the field-driven case, the transition was found to be second order so that both the order parameter u_0 and the response frequency vanish at the transition. Whenever $u_0 = 0$, (38) applies; so the conclusions of the previous paragraph are valid in this case and agree with the results shown in Fig. 12.

In the instability-driven case, the supercooling point is where the response frequency of the undistorted phase vanishes. Thus we expect that, for large χ the true transition will occur somewhat above the supercooling point and, for small χ it will occur considerably above this point. This anticipated behavior agrees with that shown in Fig. 11.

In the displaced-oscillator variational treatment of the instability-driven case, we would not only like to interpret why the transition occurs where it does, but also why it is first rather than second order. The reason for the latter is that the choice of wave functions used in the variational treatment is not the best. Part of the motive for the work in this paper was for us to gain a better understanding of the results reported in Refs. 18 and 19 for an analogous three-dimensional problem.

The displaced oscillator was chosen as the closest one-dimensional analog of the three-dimensional displaced-oscillator density matrix. Using this wave function to calculate the energy of the displaced state as a contrast to the energy of the undisplaced state has two flaws. First, Ψ_R has the wrong symmetry; to be a proper ground-state wave function it should be symmetric. Second, as is obvious from Fig. 1, in the region of low λ it is a superior variational wave function to φ_0^- and the fact that one finds a lower variational energy with this form does not necessarily imply anything about a transition.

Even though Ψ_R does not have the right symmetry, the difference between using this wave function and Ψ_0 (or Ψ_1) as defined in (8) is only of the order of the overlap $\langle \Psi_L | H^- | \Psi_R \rangle$. This quantity is of the order of magnitude of the right-hand side of (11) and, as can be noted in Fig. 4, is a rapidly decreasing function of λ as $\lambda \to 0$. Either Ψ_R, Ψ_0, or Ψ_1 yields the limiting value $E_0^- \to -1$, $\lambda \to 0$. In contrast, the limiting value obtained from the undisplaced oscillator wave function of Eq. (4) is $E_0^- \to -\frac{1}{3}$, $\lambda \to 0$. This variational form simply does not have the ability to concentrate the particle density in the region of the potential minimum even when kinetic-energy considerations permit it.

Of course, what one could do is use Ψ_0 and Ψ_1 as variational wave functions to estimate $\mathcal{E}_1^- - \mathcal{E}_0^-$ and $\langle \varphi_1^- | u | \varphi_0^- \rangle$. In this case we have already seen in Fig. 4 that energy of the symmetric state is always lower when $\chi = 0$ as it should be. However, the analogous three-dimensional treatment is much harder to visualize. For $\chi \neq 0$ we correctly obtain a second-order transition with this treatment, but the transition point is not very well determined when χ is small. This is readily understood on the basis of the two-level formula and the fact pointed out in Fig. 4 that $\mathcal{E}_1^- - \mathcal{E}_0^-$ is not very well estimated by this approach at small λ values.

An important result of this paper is implicit in (37). This equation not only is a simple expression for the determination of the transition point, but also involves only quantities which are smooth functions of λ and which can be determined reliably by means of simple variational calculations. (We assume that a suitable variational procedure will be found for the order-disorder region.) Thus, because a proper theory of the transition has been

formulated, we are able to determine the transition point without resorting to the exact, matrix-diagonalization procedure. Since the latter is equivalent to a very high-order perturbation calculation, it would be impossible in a three-dimensional system. Nevertheless, one could hope to obtain a temperature-dependent expression for a three-dimensional system in which the relevant quantities could be estimated on a first-principles basis from a microscopic Hamiltonian.

The three-dimensional analog to the present calculation is to introduce correlated Gaussian density matrices for the displaced and undisplaced states of a three-dimensional lattice.[19] In the present work we found that the variationally optimized ground-state wave function (4) provided an excellent evaluation of the ground- and first-excited-state energies of H_0^+ for all λ. Similarly, one would expect that in the absence of hard-core interactions or cubic anharmonicity the correlated Gaussian form for the density matrix of the three-dimensional lattice would provide an accurate evaluation of the free energies associated with the distorted and undistorted structures of a lattice of correlated quartic oscillators with a positive definite force-constant matrix. Furthermore, since the difference in free energies of the two structures[32] is a measure of the "soft" collective excitation associated with the structural transition, the correlated Gaussian ansatz should provide a good description of the temperature dependence of this soft mode.

If the force-constant matrix of the three-dimensional lattice is not positive definite, then the Gaussian approximation is expected to work best in the temperature region where the thermal energy of the collective mode exceeds the depth of the double well associated with this mode. This latter conclusion is a generalization of the conclusions which we reached concerning the eigenvalue spectrum of H_0^- in Sec. II. There we found that the variational treatment of H_0^- using a wave function of the form (8b) worked best for large λ; in particular, for values of λ for which the zero-point energy was such that the particle no longer felt the presence of the hump in the double well.

At this point it is perhaps appropriate to comment at greater length on the connection between λ and an effective temperature. To do this we compare the λ dependence of $\langle u^2\rangle$ with the temperature dependence of the same quantity when calculated using a single-mode classical density matrix of the type employed by Lines.[15] For definiteness, we compare the results of our variational treatment of the Hamiltonian H_0^+ using the trial ground-state wave function (8b) with a similar variational treatment using a single-mode density matrix. In the latter case, of course, we calculate the classical free energy rather than the ground-state energy. Without entering into the details of the calculation, we merely state that the resulting free-energy expression is identical to (25) with the kinetic-energy term $\frac{1}{4}\lambda^2 g$ replaced by an entropy contribution $\frac{1}{2}T\ln g$, where T is an appropriate reduced temperature. If a qualitative equivalence exists between λ and T, then we would expect that a quantity such as $\langle u^2\rangle$ calculated as a function of temperature would display a dependence on T similar to the λ dependence of the same quantity calculated within the context of the model treated in this paper. Indeed, one finds that the λ and T dependence of $\langle u^2\rangle(\lambda)$ and $\langle u^2\rangle(T)$ mirror each other quite well. In the limit of small λ or small T both $\langle u^2\rangle(\lambda)$ and $\langle u^2\rangle(T)$ display linear dependences on λ and T, respectively. Furthermore, at the second-order transition point,

$$\langle u^2\rangle(\lambda_c)=\langle u^2\rangle(T_c)=\tfrac{1}{48}(\chi-8)\,,$$

with variations about the transition point being linear in $(\lambda-\lambda_c)$ or $(T-T_c)$. Thus, we see that if we restrict ourselves to qualitative considerations only, one can safely use λ and T interchangeably. Only for large λ is the equivalence between λ and T broken. One finds that $\langle u^2\rangle(\lambda)\sim\lambda^{2/3}$, $\lambda\to\infty$, whereas $\langle u^2\rangle(T)\sim T^{1/2}$, $T\to\infty$. This departure from a strict one-to-one correspondence between λ and T is to be expected here since large λ implies large $\hbar$ and it is no longer valid to make a direct comparison with a classical temperature model. However, the difference between $\lambda^{2/3}$ dependence and the $T^{1/2}$ dependence is of no importance as far as the conclusions reached in this paper are concerned.

The exact calculation required the diagonalization of a Hamiltonian matrix. In all cases, enough exploratory numerical work was performed to guarantee the reliability of all quoted results. For most cases, a matrix of 40×40 was sufficient; however, at the lowest λ values there was considerable cancellation between $\mathcal{E}_1^-$ and $\mathcal{E}_0^-$ in order to obtain $\mathcal{E}_1^- - \mathcal{E}_0^-$ and it was necessary to use matrices up to 400×400.

APPENDIX

It is quite easy to show that, in the two-level approximation discussed in Sec. III, the displacement in the region immediately below the transition follows a square-root behavior. That is,

$$\langle u\rangle \propto (\lambda_c-\lambda)^{1/2}\,. \tag{A1}$$

In this Appendix, we will show that this behavior is a general result of the mean-field approximation providing certain symmetry conditions obtain. In order to establish this, a generalized version of the system described by the Hamiltonian (3) will be treated here. The appropriate specialized results are then easily obtained.

Suppose that $H=H(\lambda)$ is any Hamiltonian in which the kinetic-energy term is $-\frac{1}{2}\lambda^2(d^2/dx^2)$ and the potential energy $U(x)=U(-x)$ is symmetric. Then all of the eigenfunctions of H are symmetric or antisymmetric. Suppose further that U is not pathological so that all of the properties of H will be smoothly varying functions of λ. Next consider

$$\mathcal{H}=H-FV(x), \tag{A2}$$

where $V(x)$ is antisymmetric and

$$F=\chi\langle f(x)\rangle_F, \tag{A3}$$

with $f(x)$ also antisymmetric. Previously, $f(x)=V(x)=x$ has been used. The notation $\langle\ \rangle_F$ is used to indicate the average value of a quantity with respect to the ground-state eigenfunction of (A2); the subscript F is a reminder that the ground-state eigenfunction is obtained with a particular value of F in (A2). The possible states of the system described by (A2) are the self-consistent solutions of (A3). H is considered to be the unperturbed Hamiltonian and its ground-state eigenfunction will be symmetric so that $\langle f(x)\rangle_{F=0}=0$. Since the result of turning on the perturbation FV will be to lower the ground-state energy, any self-consistent solution to (A3) other than $F=0$ will result in a transition.

A graphical illustration of the above is shown in Fig. 14. The dashed straight line represents the definition $F=\chi\langle f(x)\rangle$. The solid curves (a)–(c) represent the expected functional behavior of the calculated quantity $\langle f(x)\rangle_F$ for various values of λ. Since the effect of zero-point energy gives additional rigidity to the wave function, the relationship $\lambda_a>\lambda_c>\lambda_b$ should hold. If the slope of c at the origin is $1/\chi$, the transition occurs at λ_c, and λ_a and λ_b are above and below the transition, respectively. The shape of the curves (a)–(c) will give rise to a second-order transition. The curve (d) illustrates a case in which the transition would be first order.

Thus, we see that a second-order transition requires that

$$\left.\frac{d\langle f\rangle_F}{dF}\right|_{F=0}=\frac{1}{\chi}, \tag{A4}$$

or that $\langle f(x)\rangle_F=F/\chi+$ (higher-order terms in F) at $\lambda=\lambda_c$. An additional requirement is that the $\langle f(x)\rangle_F$-vs-F curve must always lie below the straight line obtained from extrapolating the curve from its slope at the origin. If this latter behavior obtains for all λ values, the transition will be second order for any value of χ. Different behavior can result in the possibility of first- or second-order transitions for different χ values.

The functional form of $\langle f(x)\rangle_F$ can be obtained from a perturbation treatment based on the method of matrix partitioning.[33]

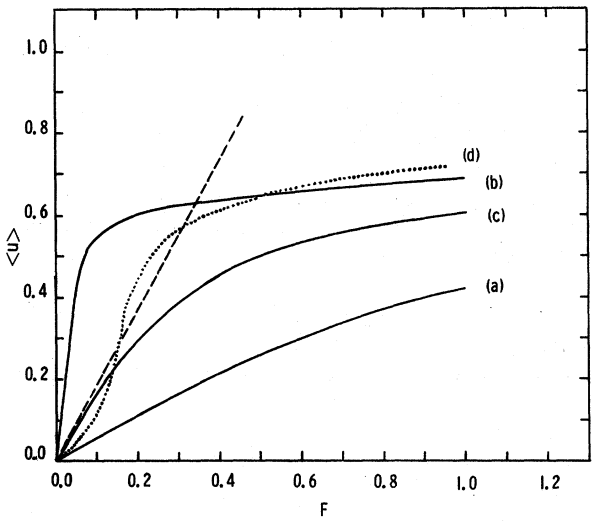

FIG. 14. Graphical illustration of the self-consistent solutions to Eq. (A3). Solutions are given by the intersection of the dashed straight line of slope χ^{-1} with the curves labeled (a)–(d). The solid curves (a)–(c) correspond to a second-order transition, whereas the dotted curve (d) illustrates a possible first-order transition.

In the representation in which H is diagonal, $\mathcal{H}$ can be partitioned as follows:

$$\mathcal{H}=\begin{pmatrix}\mathcal{H}_{00} & \mathcal{H}_{0y}\\ \mathcal{H}_{y0} & \mathcal{H}_{yy}\end{pmatrix} \tag{A5a}$$

$$=\begin{pmatrix}\mathcal{H}_{00} & \mathcal{H}_{0\mu} & \mathcal{H}_{0\nu}\\ \mathcal{H}_{\mu 0} & \mathcal{H}_{\mu\mu} & \mathcal{H}_{\mu\nu}\\ \mathcal{H}_{\nu 0} & \mathcal{H}_{\nu\mu} & \mathcal{H}_{\nu\nu}\end{pmatrix}, \tag{A5b}$$

where the subscript 0 denotes the ground-state eigenfunction of H, μ denotes all of the antisymmetric eigenfunctions, ν denotes all of the symmetric eigenfunctions except 0, and y denotes both μ and ν. Similarly, the ground-state eigenfunction of $\mathcal{H}$ can be written

$$\Psi_0=\begin{pmatrix}1\\ \Psi_y\end{pmatrix}=\begin{pmatrix}1\\ F\Psi_\mu\\ F\Psi_\nu\end{pmatrix}, \tag{A6}$$

where the factor of F is for later convenience.

The definition of the ground-state energy $\mathcal{H}\Psi_0=\mathcal{E}_0\Psi_0$ implies

$$\mathcal{E}_0=\mathcal{H}_{00}-\mathcal{H}_{0y}(\mathcal{H}_{yy}-\mathcal{E}_0)^{-1}\mathcal{H}_{y0} \tag{A7}$$

and

$$\Psi_y=-(\mathcal{H}_{yy}-\mathcal{E}_0)^{-1}\mathcal{H}_{y0}. \tag{A8}$$

From the choice of basis functions and symmetry conditions, H is diagonal and V and f only have matrix elements between states of opposite symmetry. Thus

$$\mathcal{H}=\begin{pmatrix}E_0 & -FV_{0\mu} & 0\\ -FV_{\mu 0} & E_\mu & -FV_{\mu\nu}\\ 0 & -FV_{\nu\mu} & E_\nu\end{pmatrix} \tag{A9}$$

and

$$f=\begin{pmatrix} 0 & f_{0\mu} & 0 \\ f_{\mu 0} & 0 & f_{\mu\nu} \\ 0 & f_{\nu\mu} & 0 \end{pmatrix}, \tag{A10}$$

where E_μ and E_ν are written with single subscripts to indicate that they are diagonal. One can combine (A6) and (A9) to obtain

$$\langle f\rangle_F = 2F\,\frac{f_{0\mu}\Psi_\mu + F\Psi_\nu f_{\nu\mu}\Psi_\mu}{1+F^2\Psi_\mu^2+F^2\Psi_\nu^2} \tag{A11}$$

and can use (A8) together with the matrix elements exhibited in (A9) to obtain

$$\begin{pmatrix}\Psi_\mu\\ \Psi_\nu\end{pmatrix}=\begin{pmatrix} E_\mu-\underset{\sim}{\mathcal{E}}_0 & -FV_{\mu\nu} \\ -FV_{\nu\mu} & E_\nu-\underset{\sim}{\mathcal{E}}_0\end{pmatrix}^{-1}\begin{pmatrix}V_{\mu 0}\\ 0\end{pmatrix} \tag{A12}$$

$$=\begin{bmatrix}(M^{-1})_{\mu\mu} & V_{\mu 0}\\ (M^{-1})_{\nu\mu} & V_{\mu 0}\end{bmatrix}, \tag{A13}$$

where $\underset{\sim}{\mathcal{E}}_0$ has been used to designate $\mathcal{E}_0$ times the identity matrix of appropriate dimension and M is used to represent the matrix in (A12).

Next, one can use two relationships between the partitioned components of any matrix M and the components of its inverse:

$$(M^{-1})_{\mu\mu}=[M_{\mu\mu}-M_{\mu\nu}(M_{\nu\nu})^{-1}M_{\nu\mu}]^{-1} \tag{A14}$$

and

$$(M^{-1})_{\nu\mu}=-(M_{\nu\nu})^{-1}M_{\nu\mu}(M^{-1})_{\mu\mu}\,. \tag{A15}$$

Now if, for notational convenience, we define

$$D_{\mu\mu}=(M^{-1})_{\mu\mu}$$
$$=[E_\mu-\mathcal{E}_0-F^2V_{\mu\nu}(E_\nu-\mathcal{E}_0)^{-1}V_{\mu\nu}]^{-1}, \tag{A16}$$

the components of the ground-state wave function are found to be

$$\Psi_\mu = D_{\mu\mu}V_{\mu 0} \tag{A17}$$

and

$$\Psi_\nu = F(E_\nu-E_0)^{-1}V_{\nu\mu}\Psi_\mu\,. \tag{A18}$$

Since $\mathcal{E}_0 < E_0$ and all of the energies represented by E_μ and E_ν must be greater than E_0, $(E_\mu-\mathcal{E}_0)^{-1}$ and $(E_\nu-\mathcal{E}_0)^{-1}$ must exist and a Taylor-series expansion of (A16) about $F=0$ can be made. The key point is that $D_{\mu\mu}$ and therefore Ψ_μ are both of the form constant plus a series in F^2.

The expressions (A11), (A17), and (A18) can now be combined to obtain

$$\langle f\rangle_F = 2F\,\frac{f_{0\mu}\Psi_\mu + F^2\tilde{\Psi}_\mu V_{\mu\nu}(E_\nu-\mathcal{E}_0)^{-1}f_{\nu\mu}\Psi_\mu}{1+F^2\tilde{\Psi}_\mu[1+F^2V_{\mu\nu}(E_\nu-\mathcal{E}_0)^{-2}V_{\nu\mu}]\Psi_\mu}\,. \tag{A19}$$

From the considerations of the previous paragraph, it is clear that $\langle f\rangle_F$ can be written as $F\times$(power series in F^2). The coefficients in the power series should be smooth functions of λ since they involve only quantities which are themselves expected to be smooth functions of λ. In the vicinity of a second-order transition, this expression must be of the form

$$\langle f\rangle_F=[\chi^{-1}+b_1(\lambda_c-\lambda)]F-b_2F^3\,, \tag{A20}$$

where the coefficients in the series have been expanded in powers of $(\lambda_c-\lambda)$ and only the essential dependence on this quantity has been retained. The form of the linear term is dictated by (A4). The coefficients b_1 and b_2 are constants. Now, if (A20) is combined with (A3), two self-consistent solutions for $\langle f\rangle_F$ are found,

$$\langle f\rangle_F = 0 \tag{A21}$$

or

$$\langle f\rangle_F=\chi^{-1}(b_1/b_2)^{1/2}(\lambda_c-\lambda)^{1/2}\,. \tag{A22}$$

The first is trivial; the second gives the required square-root behavior.

It should be emphasized that the initial assumptions that H is even and that f and V are odd are responsible for the elimination of all terms involving even powers of F in the power-series expansion of $\langle f\rangle_F$.

One can obtain an explicit expression for χ by combining (A4) and (A19). In the notation used in this Appendix, the expression is

$$\chi^{-1}=2f_{0\mu}(E_\mu-E_0)^{-1}V_{\mu 0}\,, \tag{A23}$$

where E_0 rather than $\mathcal{E}_0$ appear because $E_0=\mathcal{E}_0$ at the transition. If we return to the notation used in the main text,

$$\chi^{-1}=2\sum_\alpha \langle\varphi_\alpha^\pm|u|\varphi_0^\pm\rangle^2/(\mathcal{E}_\alpha^\pm-\mathcal{E}_0^\pm) \tag{A24}$$

results, in agreement with expression (33) for the vanishing of the response frequency.

The result (A19) serves as a starting point for an investigation of conditions under which the transition might be first order. However, such considerations will be postponed until later.

*Work supported by the U. S. Atomic Energy Commission.

[1]R. Blinc, J. Phys. Chem. Solids **13**, 204 (1960).
[2]P. G. de Gennes, Solid State Commun. **1**, 132 (1963).
[3]R. Brout, K. A. Müller, and H. Thomas, Solid State Commun. **4**, 507 (1966).
[4]J. Villain and S. Stamenkovic, Phys. Status Solidi **15**, 585 (1966).
[5]M. Tokunaga, and T. Matsubara, Prog. Theor. Phys. **35**, 581 (1966).
[6]M. Tokunaga, Prog. Theor. Phys. **36**, 857 (1966).
[7]K. K. Kobayashi, J. Phys. Soc. Jap. **24**, 497 (1968).
[8]P. W. Anderson, in *Fizika Dielektrikov*, edited by G. I. Skanavi (Akademica Nauk SSSR Fisicheskii Inst. im P. N. Lebedeva, Moscow, 1960).
[9]W. Cochran, Adv. Phys. **9**, 387 (1960).
[10]B. D. Silverman and R. I. Joseph, Phys. Rev. **129**, 2062

(1963); R. I. Joseph and B. D. Silverman, Phys. Rev. **133**, A207 (1964).

[11]B. D. Silverman, Phys. Rev. **135**, A1596 (1964).

[12]R. A. Cowley, Philos. Mag. **11**, 673 (1965).

[13]A. A. Maradudin, in *Ferroelectricity*, edited by E. F. Weller (Elsevier, Amsterdam, 1967).

[14]P. C. Kwok and P. B. Miller, Phys. Rev. **151**, 387 (1966).

[15]M. E. Lines, Phys. Rev. **177**, 797 (1969); Phys. Rev. **177**, 812 (1969); Phys. Rev. **177**, 819 (1969); Phys. Rev. B **2**, 690 (1970); Phys. Rev. B **2**, 698 (1970).

[16]Y. Onodera, Prog. Theor. Phys. **44**, 1477 (1970); Prog. Theor. Phys. **45**, 986 (1971).

[17]N. Boccara and G. Sarma, Physics (N.Y.) **1**, 219 (1965).

[18]N. S. Gillis and T. R. Koehler, Phys. Rev. B **4**, 3971 (1971).

[19]N. S. Gillis and T. R. Koehler, Phys. Rev. B **5**, 1925 (1972).

[20]E. Pytte and J. Feder, Phys. Rev. **187**, 1077 (1969); and J. Feder and E. Pytte, Phys. Rev. B **1**, 4803 (1970).

[21]Michael Cohen and Theodore L. Einstein, Phys. Rev. B **7**, 1932 (1973).

[22]E. Pytte, Phys. Rev. B **5**, 3758 (1972).

[23]The mean-field Hamiltonian (2) is a rigorously valid description of the system of coupled oscillators in the limit of an infinitely long-range and infinitely weak intercell interaction; W. J. Camp, private communication. In particular, this requires that $\chi(ll') = \chi(q = 0)/N$, $N \to \infty$, where $\chi(q = 0)$ is the long-wavelength Fourier component of $\chi(ll')$.

[24]P. B. Miller and P. C. Kwok, Phys. Rev. **175**, 1062 (1968).

[25]A preliminary account of this work has been given in N. S. Gillis and T. R. Koehler, Phys. Rev. Lett. **29**, 369 (1972).

[26]In principle, one should minimize $\langle \psi_0|H^-_0|\psi_0\rangle / \langle \psi_0|\psi_0\rangle$ rather than $\langle \psi_L|H^-_0|\psi_L\rangle$. However, these two quantities differ only by terms of the order of the overlap $\langle \psi_L|\psi_R\rangle$, and this is numerically quite small.

[27]For a review of the literature concerning the self-consistent phonon approximation as applied to the anharmonic properties of crystals see N. R. Werthamer, Am. J. Phys. **37**, 763 (1969).

[28]We must be careful to add a term $\chi u_0^2/2$ to $H^+(u)$ to avoid overcounting the interactions when the ground-state average of $H^+(u)$ is taken.

[29]A detailed consideration of the linear response of a crystal lattice to an external perturbation within the context of the Hartree approximation is given in D. R. Fredkin and N. R. Werthamer, Phys. Rev. **138**, A1528 (1965), and in Ref. 24.

[30]See, for example, L. P. Kadanoff and G. Baym, *Quantum Statistical Mechanics* (Benjamin, New York, 1962), Sec. 6.2.

[32]This free-energy difference is the finite-temperature counterpart of the energy difference $E_1 - E_0$ considered in the present paper. The analog of the energy E_1 is the free energy associated with a density matrix appropriate to the distorted structure. On the other hand, E_0 corresponds to the free energy of the undistorted structure, calculated using a symmetric density matrix.

[33]P. O. Lowdin, J. Math. Phys. **3**, 969 (1962).